TOPICAL REVIEW — Magnetism, magnetic materials, and interdisciplinary research

Progress in organic spintronics*

Yang Fu-Jiang(杨福江), Han Shi-Xuan(韩士轩), and Xie Shi-Jie(解士杰)†

School of Physics, State Key Laboratory of Crystal Materials, Shandong University, Jinan 250100, *China*

(Received 28 February 2014; published online 25 March 2014)

Recent progress in organic spintronics is given an informative overview, covering spin injection, detection, and transport in organic spin valve devices, and the magnetic field effect in organic semiconductors (OSCs). In particular, we focus on our own recent work in spin injection and the organic magnetic field effect (OMFE).

Keywords: organic material, spintronics, spin injection, organic magnetic field effect

PACS: 81.05.Lg, 85.75.–d, 75.47.–m **DOI:** 10.1088/1674-1056/23/5/058106

1. Introduction

In recent years, the field of organic spintronics has seen great progress, both experiment and theory. The increased motivation comes from the unique advantages of organic semiconductors, including flexibility, low weight, and low-cost fabrication, as well as from the strong technical support recently emerging in the fields of chemistry and material science.

As the enabling carrier for message storage and transport, an electron has two aspects: charge and spin. In normal electronic devices, they are used separately. For example, integrated circuit devices carry messages based on the electronic charges, while diskettes store messages based on the electronic spins. However, the discovery of giant magnetoresistance (GMR) and tunneling magnetoresistance (TMR) in metallic spin valves has revolutionized applications such as magnetic recording and memory, and has launched a new field of spin electronics — spintronics[1–3] — which is centered on the electron spin, including its generation, transport, and detection. The recent employment of spin freedom in applications enriches microelectronics and makes it possible to fabricate many novel devices.

The initial work on spintronics is to study the possibility of spin transport in nonferromagnetic materials. So far, based on heterostructures or sandwich structures, spin injection and transport in superconductors, metals, and semiconductors have been widely studied.[4–6] Most investigations have concentrated on the current-induced spin polarization in semiconducting devices. Since organic functional materials have the characteristics of semiconductors, it is natural to consider an alternative to normal semiconductors: the organic semiconductors.

Unlike the normal inorganic semiconductor materials, organic semiconductors (OSCs) are easily synthesized and processed at room temperature. It is well known that organic small molecules and polymers have many interesting electronic, magnetic, and optical properties. Organic light-emitting diodes (OLEDs) for flat-screen TVs, cell phone displays, billboards, and computer displays have been fabricated.[7–9] In addition, OSCs have extremely weak spin–orbit coupling and weak hyperfine interaction, so the electron spin diffusion length is especially long.[3] These properties make them ideal for spin-polarized injection and transport applications, which are anticipated to be the next hot topic in spintronics. Organic spintronics not only broadens our understanding of the physical world of organic materials but also has a substantial impact on spintronic and bionomic applications. A comprehensive review of organic spintronics, addressing both theoretical and experimental aspects, appeared in 2007, which covered the major results published up to that date.[10] A later article reviewed the major experimental results.[11] In addition, a brief overview of the first eight years of spin transport research in OSCs was given by Kazi and Sandipan.[12] In 2006 and 2009, we made two efforts to summarize the progress in organic spintronics at those dates, which appeared as chapters in two books, *Progress in Ferromagnetism Research* and *Advances in Condensed Matter Physics*.[13,14]

The present article is organized as follows. In Sections 2 and 3, we review OSCs and spintronics, which are presented separately. In Section 4, the progress in organic spin injection and transport, and the developments in organic magnetic field effect (OMFE) are described. Finally, in Section 5, a summary is given.

2. Organic semiconductors

Organic spintronics include OSCs and spintronics. OSCs contain small molecules as well as polymers. Small molecules

*Project supported by the National Basic Research Program of China (Grant No. 2010CB923402), the National Natural Science Foundation of China (Grant Nos. 11174181 and 21161160445), and the 111 Project, China (Grant No. B13029).

†Corresponding author. E-mail: xsj@sdu.edu.cn

© 2014 Chinese Physical Society and IOP Publishing Ltd

such as tris(8-hydroxyquinolinato)aluminium (Alq_3) and pentacene are widely used to fabricate organic devices because these materials may have a high carrier mobility and have readily apparent functional properties. Variations in the substituents in the quinoline rings enrich the performance of these devices. In 1976, Heeger *et al.* synthesized polyacetylene and tuned its conductance by doping.[15] From then on, thousands of organic conjugated polymers or organic materials, such as polythiophene (PT), polyparaphenylene (PPP), and polyacetylene (PA), have been synthesized. The conductance of these polymers covers the range from insulating, semiconducting, to metallic.

In 1987, Tang and Slyke were the first to demonstrate a low-voltage and efficient thin-film LED and opened the door to using organic small molecules for a new generation of optoelectronic devices.[16] In 1990, Burroughes *et al.* obtained organic electroluminescent devices with common organic polymer poly phenylene vinylene (PPV).[17] From then on, OLEDs and organic field-effect transistors (OFETs) were rapidly developed.[18–20] These devices are currently being incorporated into a variety of displays and are also potentially important for a wide range of other applications. Jiang *et al.* presented a theoretical design of poly(thienylene vinylene) (PTV) derivatives for the improvement of the performance of light-emitting and photovoltaic devices. They predicted that carbonyl-substituted PTV is a strongly fluorescent polymer with low bandgap, long exciton lifetime, and large spectral overlap between emission and absorption.[21]

In addition to the electrical and optical properties of organic materials, it was also found that OSCs may show ferroelectricity and ferromagnetism. As early as 1968, Mataga proposed that new organic magnets could be based on π-conjugated polymers.[22] Ovchinnikov *et al.*[23] and Cao *et al.*[24] separately synthesized an organic ferromagnet called poly-BIPO. Significant progress has been made in the preparation of π-conjugated oligomers and polymers with large values of spin quantum number, and organic polymer magnets have remained a great challenge that has attracted considerable attention.[25–27] Therefore, it seems that all the functional properties, such as electricity, magnetism, photonics and even caloritronics could be realized in organic materials. It is expected that an all-organic functional device will be manufactured in the near future. Due to their pioneering work in organic polymers, Heeger, MacDiarmid, and Shirakawa shared the Nobel Prize for chemistry in 2000.

Organic polymers, such as polyacetylene, are representative of organic functional materials. They usually have a highly conjugated structure with a quasi-one-dimensional chain characteristic. Strong electron–lattice interactions are their important characteristics, which are different from those of normal inorganic materials. Because of the strong intrachain bonding and the weak interchain interaction characteristics, π electrons are delocalized, principally along the polymer chain. A pristine polymer, such as polyacetylene, is a semiconductor or insulator depending upon the gap width between the highest occupied molecular orbital (HOMO) and the lowest unoccupied molecular orbital (LUMO). But when it is doped or charge injected, the structure and the properties of a polymer may be changed dramatically. An extra electron (or hole) will be trapped to form a charged soliton or polaron. It is also discovered that two charged polarons can attract each other to form a bipolaron. All of these excitations are localized in a spatial structure that is induced by the strong electron–lattice coupling in conjugated polymers. In 1979, Su, Schrieffer, and Heeger gave a simple tight-binding model to describe the ground state and the excitations in polyacetylene, which is well known as the SSH model.[28–30] They pointed out that solitons, polarons, or bipolarons in conducting conjugated polymers behave as quasi-particles with complete localization, stability, and integrity. In some small-molecule crystals, it was also indicated that, due to the molecular fluctuation around the equilibrium position, an extra electron (hole) will form a self-trapped state, which is similar to a charged excitation in a polymer.[31]

Most important is the special charge–spin relationship in these excitations in OSCs, as shown in Table 1. A soliton has a reverse charge–spin relation, which is different from the conventional electron or hole carrier; that is, a charged soliton $S^{\pm}$ is spinless, but a neutral soliton S^0 has a spin $\pm\hbar/2$. A charged polaron carries spin $\pm\hbar/2$. A bipolaron binds two electrons or holes, so it is spinless. Apparently, only charged polarons or neutral solitons can serve as spin carriers.

Table 1. Charge–spin relations of soliton, polaron, and bipolaron.

Excitation	Charge/e	Spin/$\hbar$
Soliton	0	$\pm1/2$
	±1	0
Polaron	±1	$\pm1/2$
Bipolaron	±2	0

In 2010, Tarafder *et al.* theoretically studied the spin polarization of charged carriers — any charged carriers — in an Alq_3 molecule by using the density functional theory (DFT) method.[32] They found that the injected charges have a lower energy in a spin-polarized state than that in a non-polarized state. The polarization or magnetic moment increases nearly linearly with the injected charge quantity. Alq_3 contains a metal atom, which makes it difficult to elucidate the reason for the charge induced polarization, so we studied this question with pure organic oligothiophene.[33,34] It was found that the charges will accumulate to form a localized wavepacket. If the charge quantity is one electronic unit, it is a polaron (as mentioned above). If the charge quantity is two electronic units,

it is a bipolaron. Although the wavepacket is spin-polarized, the polarization characteristic in the polymerized oligomer is different from that in small molecule Alq_3. The emergence and variation of the net magnetic moment are related to both the amount of charge injected and the polymerization of the oligomer, as shown in Figs. 1 and 2, respectively.[33,34] It was found that the strong electron–phonon (e–ph) coupling belonging to organic materials is critical for the emergence of spin polarization. The polarization intensity or magnetic moment is dependent on the amount of injected charges and the polymerization of the molecule.

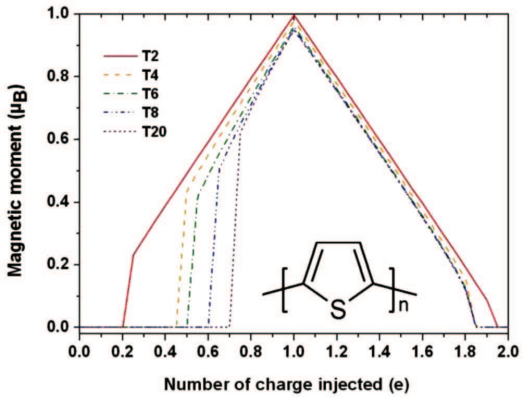


Fig. 1. Magnetic moment as a function of injected electron charge in thiophene from oligomer to polymer. The inset shows the molecular structure of thiophene oligomer.

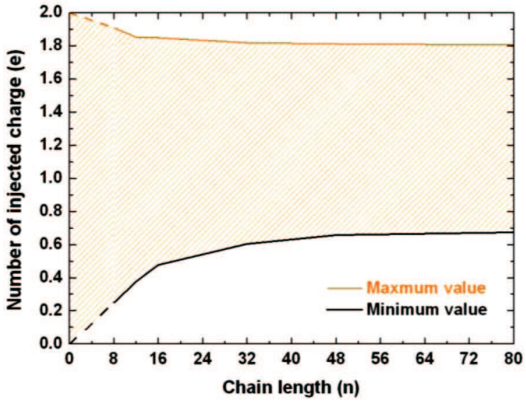


Fig. 2. Dependences of the minimum and the maximum charges for the emergence (disappearance) of the net magnetic moment in oligomer polymerization.

OSCs have caught the attention of the spintronics community since 2002, and significant efforts are being made toward their integration in this field.[35] OSCs' most attractive aspect for spintronic applications is the weakness of their spin-scattering mechanism, which implies that the spin polarization of the carriers can be maintained for a very long time. This property is due to the very light atomic mass constructing the organic materials or the weak spin–orbit coupling. Notably, a spin-relaxation time of more than 10 μs was obtained, which exceeds the characteristic time in inorganic materials by an order of magnitude. At present, organic spintronics can be regarded as a fascinating puzzle for which many pieces are still missing. Although a lot of attractive phenomena have been found in OSCs and organic devices, the field is not progressing as swiftly as it could because of a recent proliferation of physical models of spin-dependent properties, models which are tailored to specific data.[36]

The electronic properties of OSCs are radically different from those of their inorganic counterparts with rigid band structures. Consequently, their spin properties are also different. In band semiconductors, spin injection and transport are commonly described by considering either ballistic or diffusive motion of spin-polarized carriers in delocalized band states. The spin-flipping processes proceed mainly via the spin–orbit coupling, which can transform the scattering of the angular momentum into spin scattering. OSCs are composed of small molecules and polymers, both of which have spatial molecular structures. In a molecular crystal or within a polymer chain, the transport may be approached with the band-like theory to some extent. However in an amorphous molecular structure or among polymer chains, the transport is incoherent. Hopping dominates the transport. Therefore, precisely speaking, OSCs are not characterized by band conductivity, nor do they feature a significant spin–orbit coupling. The charge carriers contain spin polarons as well as spinless bipolarons. These carriers propagate in an OSC by incoherent hopping between strongly localized states. Unveiling the fundamental aspects of these materials is, therefore, what makes the field simultaneously challenging and exciting.

3. Spintronics

In 1996, Wolf introduced the word "spintronics." [3] The discovery of GMR in 1988 is considered to be the first work in this area.[1] Fundamental studies of spintronics include investigations of spin transport in electronic materials, as well as spin dynamics and spin relaxation.[3,37]

A ferromagnetic/interlayer/ferromagnetic sandwich structure is the basic configuration in the studies of spin-polarized injection and transport. The nonmagnetic interlayer may be superconductor, metal, conventional semiconductor, organic material, *etc*. When a superconductor is used as the interlayer, it is impossible to achieve spin transport because the carriers in the superconductor are spinless Cooper pairs. Studies in these fields focus on the separation of the electron and the spin in superconductors.[38] Carriers in metals are well-extended electrons which carry 1/2 spin. Therefore, metals can be used as spin injection and transport materials. However, metal devices cannot amplify the signals, so the metals' applications are restricted. The carriers in semiconductors are either electrons or holes, and both have 1/2 spin. Semiconductors are most suitable for spintronics and

for amplifying the signals because of the existence of the bandgap. Organic polymers are another option due to their semiconducting properties. Of course, a polymer has its own characteristic: the "soft" atomic configuration makes it easily form a well-contacted interface or an adjustable injection barrier. The special charge–spin relations make organic materials different from normal semiconductors.

One important quantity characterizing spin polarization transport in spintronics is the current spin polarization, defined as[39]

$$P = \left(J_\uparrow - J_\downarrow\right) / \left(J_\uparrow + J_\downarrow\right), \tag{1}$$

where J_s ($s = \uparrow, \downarrow$) corresponds to the current density with spin s. For a ferromagnetic/semiconductor/ferromagnetic trilayer, the spin diffusion theory tells us that the current spin polarization of the system is sensitively related to the conductivities in the ferromagnetic layer and the contact layer. A remarkable current spin polarization can be achieved with a suitable conductivity match. This has motivated the many investigations into ferromagnetic semiconductors because this trilayer has the characteristics of both ferromagnetism and semiconduction. One example is the widely used half-metallic material $La_{1-x}Sr_xMnO_3$. Magnetic semiconductor materials have extraordinarily complicated characteristics and structures. Magnetic semiconductors have been used in spin injection experiments.[40] The progress in spintronics also promotes studies of the important magnetic semiconductor materials.

Another quantity that is important in understanding spintronics is the spin relaxation time τ_s or spin lifetime, given by $\tau_s^{-1} = \tau_{\uparrow\downarrow}^{-1} + \tau_{\downarrow\uparrow}^{-1}$, with the spin flip time $\tau_{ss'}$ indicating the average time for spin s to flip to spin s'. The spin relaxation time is a key parameter in spintronic devices because it sets the time scale — and hence the length scale — for the loss of spin polarization. Correspondingly, the spin relaxation length l_s is defined as the electron travel distance within time τ_s. For a semiconductor in the non-degenerate regime, l_s is given by $l_s = \left(\frac{k_B T \tau_s}{2ne^2\rho_N}\right)^{1/2}$, where n is the carrier density and ρ_N is the resistivity.[41] By using electron paramagnetic resonance measurements, room-temperature spin relaxation times in OSCs are found to be in the range of 10^{-7}– 10^{-5} s,[42] which is much longer than the 10^{-10} s relaxation time of metals.[43] A more detailed introduction to spintronics can be obtained in the review article[37] written by Zutic *et al.* and the book[44] (in Chinese) edited by Zhai *et al.*

To understand the mechanism of spin transport or that of spin polarization, let us consider the possible spin-related interactions. An electron experiences different kinds of spin-spin interactions in spintronics. The first is the direct magnetic dipole–dipole interaction. Its intensity is usually in 1 K, which is very weak. The second is the interaction of a spin and an external magnetic field, whch is the well known Zeeman effect in atomic physics. This interaction leads to the spin precession around the external magnetic field. The third is the spin–spin interaction, the Heisenberg interaction, which is induced by the Pauli blockade, the phenomenon described by the Pauli exclusion principle. The Heisenberg interaction is the origin of the ferromagnetism of materials. The fourth is the hyperfine interaction between the electron and the nuclear spin. In some semiconductors, the lattice nuclear spin exists, and a hyperfine interaction will be detectable. Some investigations have revealed that hydrogen nuclear spins are critical for the appearance of organic magnetoresistance (OMAR).

The fifth spin-related interaction is the spin–orbit coupling, which is actually a relativistic effect. An electron moving in an electric field feels an effective magnetic field $\boldsymbol{B} = (\boldsymbol{v}/c) \times \boldsymbol{E}$. This field, depending on the orbital motion of the electron, interacts with the electron's spin. This spin–orbit coupling is considerable in the case of heavy atoms. This is the well-known Rashba spin–orbit coupling for a two dimensional electron gas in semiconductor spintronics[45,46]

$$H_R = \frac{\hbar}{m_e} k_{so} (\boldsymbol{\sigma} \times \boldsymbol{p}) \cdot \boldsymbol{e}_z, \tag{2}$$

where $\boldsymbol{\sigma}$ is the Pauli matrix, $\boldsymbol{p}$ is the electron momentum, $\boldsymbol{e}_z$ is the unit vector of the electrical field, and k_{so} is the controllable parameter of the situation.

An example of a device based on the spin–orbit coupling is the Datta–Das spin field-effect transistor. In 1990, Datta and Das were first to proposed a spin field-effect transistor (SFET).[47] The Datta–Das SFET comprises a drain, a source, a narrow channel, and a gate for controlling the current. The source and the drain are ferromagnets acting as the injector and the detector of the electron spin. The source injects electrons with spins parallel to the transport direction. The electrons are transported ballistically through the channel. When they arrive at the drain, their spins are detected. In a simplified picture, the electron can enter the drain (ON) if its spin points at the same direction as the spin of the drain. Otherwise, it is scattered away (OFF). The role of the gate is to generate an effective magnetic field, arising from the spin–orbit coupling in the substrate material, from the confinement geometry of the transport channel, and the electrostatic potential of the gate. This effective magnetic field governs the processing of the electron spins. By adjusting the voltage of the gate, one can change the precession to lead to either parallel or antiparallel electron spin at the drain, effectively controlling the current.[37]

The Lorentzian interaction between a moving charge and an applied magnetic field should be mentioned, although it is not directly related to the carrier spin. An immediate result of

the Lorentzian interaction in semiconductors is the Hall effect. To understand the magnetoresistance (MR) in a nonmagnetic organic device, we have proposed a mechanism based on the Lorentzian interaction, which will be described later.

4. Organic spintronics

In this section, we will review the progress in organic spintronics during the past ten years, and pay attention to two aspects: the spin injection and transport in an organic device with ferromagnetic electrodes, and the MR in a nonmagnetic organic device. So far, no reports on all-organic spintronic devices have appeared becuase only hybrid structures with inorganic electrodes and organic active interlayers have been investigated. Nevertheless, for the sake of simplicity, we will call such hybrid devices organic spintronic devices throughout this paper.

4.1. Spin injection and transport in organic devices

In 2002, Dediu *et al.* first reported their work on an organic sandwich device. They observed the spin injection into thin films of the conjugated organic material sexithienyl (T_6) at room temperature.[48] The colossal MR manganite $La_{0.7}Sr_{0.3}MnO_3$ (LSMO) was used as the magnetic electrode. A schematic diagram of the hybrid junction is shown in Fig. 3. Two LSMO planar structure electrodes, separated by a channel of length w, were fabricated by electron-beam lithography. Each LSMO film contained six electrically separated couples of electrodes with different lengths w ranging from 70 nm to 500 nm. T_6 thin films (100–150 nm thick) were deposited by molecular beam deposition in order to cover the channel separating the electrodes and create an electrical connection between them. In the absence of an external magnetic field, the electrodes had random spin orientations. Applying a magnetic field would make the spins in the electrodes parallel. A negative MR was found, which indicates both spin-polarized injection and spin-polarized coherent transport between the electrodes. From the experimental results, they estimated the room temperature spin relaxation length in T_6 to be 200 nm.

In 2004, Xiong *et al.* built an organic spin valve (OSV). They chose the small π-conjugated molecule Alq_3 to serve as an organic spacer, which was sandwiched between layers of cobalt and half-metallic manganite LSMO.[49] After engineering the two ferromagnetic electrodes to have different coercive fields, their magnetization directions would have either a parallel or anti-parallel alignment configuration under a sweeping external magnetic field. A spin-polarized electrical current flowed from LSMO through the organic spacer (Alq_3) to Co when a positive bias V was applied. An in-plane magnetic field was swept to switch the magnetization directions of the two FM electrodes separately. The measured MR could be as high as 40% at low temperature. A line was fit through the experimental data by using the following equation based on the spin diffusion model:

$$\frac{\Delta R}{R} = \frac{R_{\mathrm{AP}} - R_{\mathrm{P}}}{R_{\mathrm{AP}}} = \frac{2P_1P_2\,\mathrm{e}^{-(d-d_0)/l_{\mathrm{s}}}}{1+P_1P_2\,\mathrm{e}^{-(d-d_0)/l_{\mathrm{s}}}}, \tag{3}$$

where P_1 and P_2 are the spin polarizations of the two electrodes, respectively. Their findings suggested that the organic spacers may be composed of two sublayers: one sublayer immediately below the Co electrode that contains Co inclusions owing to the interdiffusion (whose thickness is d_0); and a second sublayer of Alq_3 neatly deposited between this defected sublayer and the LSMO film. Their experiments produced an evidence of self-adjustment of organic materials at interfaces. The same group also studied magnetic-field-dependent carrier injection at LSMO and organic interfaces.[50] Owing to the uniqueness and ease of organic-material device fabrication, which does not need lattice matching, ferromagnetic/organic hybrid structures may be readily used to study the field effects on the electronic structures of other exotic ferromagnetic materials.

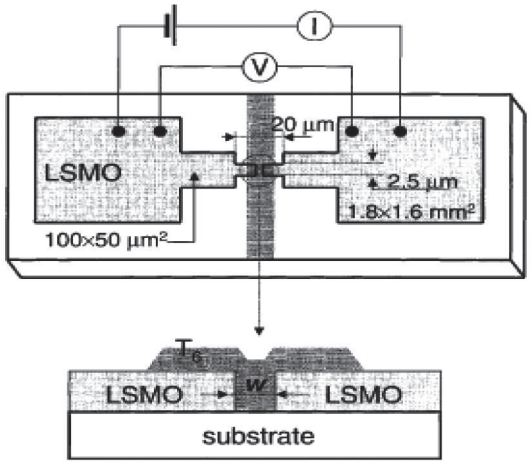


Fig. 3. Schematic diagram of a hybrid junction (drawing not to scale) and dc four-probe electrical scheme. The cross sectional view indicates the region near the spin transport channel.[48]

In 2006, Majumdar *et al.* reported the fabrication and characterization of a polymeric spin valve with regioregular (poly 3-hexylthiophene) (RRP3HT) as the spacer layer.[51] The device structure was LSMO/RRP3HT/Co. The spin valve showed a behavior similar to a magnetic tunnel junction, but the organic spacer ($\sim$ 100 nm) was much thicker than the tunneling limit. They attributed this behavior to the formation of a thin spin-selective tunneling interface between LSMO and RRP3HT caused by RRP3HT chemically attaching to LSMO as observed in X-ray photoelectron spectroscopy. They found that, by introducing monolayers of different organic insulators between LSMO and RRP3HT, the spin-selective interface is destroyed and the spin injection is reduced. Their results

showed that organic polymers are promising candidates for spintronics applications.

To enlarge the MR effect, Dediu *et al*. fabricated a device LSMO/Alq_3/Al_2O_3/Co by inserting an Al_2O_3 insulating layer between the FM contact and Alq_3. The device showed the MR effect at room temperature.[52] Mooser *et al*. improved the structure of the device and fabricated an organic spin valve device Si/SiO_2/Pt/CoPt/TIPS-pentacene/AlO_x/Co/Al. They found that it was easy to find the MR effect at room temperature.[53] Chen *et al*. also improved the OSV's MR effect by using the controlled fabrication process. For example, the LSMO bottom electrodes were annealed to obtain an atomically smooth surface and improve the magnetic properties.[54] In addition, the organic spin valve device made of C_{60} was developed. At room temperature, the MR of this device reached up to 5%.[55]

In 2009, two experiments claimed the direct observation of spin injection and transport in organic interlayers. Cinchetti *et al*. directly measured the spin injection at a ferromagnet /organic interface by using a spin-resolved two-photon photoemission method.[56] Drew *et al*. used the low-energy muon spin rotation method to measure the spin injection at a ferromagnet/organic interface, both with and without the tunnel barrier LiF.[57] Yu quantitatively explained the temperature dependent spin diffusion in Alq_3 from recent muon measurements.[58]

In a pioneering work, Mott provided a basis for understanding the spin-polarized transport.[59,60] He realized that in the case of vanishable magnon scattering, electrons of majority and minority spin do not mix in the scattering processes. The conductivity can then be expressed as the sum of two independent and unequal parts for two different spin projections. This is known as the two-current model. It provides a basic explanation for various magnetoresistance phenomena.[37] Although we can qualitatively understand the current spin polarization of an organic device by borrowing the picture of a normal semiconductor device, some characteristics of the organic materials, such as the self-adjusting interface with the ferromagnetic metals, the weak spin–orbit coupling, and the special carriers in OSCs mentioned above, should be considered in more detail. For example, in nondegenerate organic materials, the carriers are polarons and bipolarons with different charge–spin relations. These carriers can be seen as quasi-particles and described by the spin diffusion theory. The special charge–spin relation of the carriers in organic materials may play a key role in organic spintronics. Theoretical studies on spin-polarized injection and transport in organic materials include two aspects: quantum theory and classical transport equation. Microcosmic quantum theory is focused on the molecule structure, the carrier characteristics, and the spin transport dynamics. The classical theory is based on the spin diffusion equation and the Ohm's law. Both have been developed to understand the experimental results and reveal new phenomena in the organic spintronics.

4.1.1. Spin injection

Understanding the charge–spin relation or carrier properties in OSCs is the first step to investigate spin injection and transport in organic devices. Although most properties of soliton, polaron, and bipolaron have been well known, the creation, annihilation, and transition, especially the spin-related properties of these excitations, are still an interesting topic in the organic polymer area; for example, the interesting photo-induced polarization inversion and charge flipping.[61] Under photo excitation, a reaction $p_s^+ + h\nu \rightarrow p_s^- + bp^{++}$ may take place, which means that, after photo excitation, the positive polaron is decomposed into a negative polaron and a positive bipolaron. The negative polaron is driven into polymer *B* under the field while the bipolaron is left in polymer *A*. During the process, the spin moves from one polymer to another. Therefore, one may design a photo-control valve or switch of spin injection from the charge reverse of the spin carriers.

In 2003, we theoretically investigated the polarization properties of CMR material and polymer interfaces.[62] A one-dimensional nondegenerate Su–Schrieffer–Heeger Hamiltonian was used to describe the conjugated polymer and a one-dimensional tight-binding model was used to describe the ferromagnetic metal CMR. With the transfer of electronic charges and spins from the ferromagnetic electrode to the polymer, it was found that the electron (hole) density in the polymer near the interface is spin-polarized. The spin density oscillates and decays into the polymer and finally disappears. By adjusting the relative chemical potential of the contact and the polymer, electrons (holes) are injected into the polymer from the ferromagnetic electrode through the interfacial coupling and the injected electrons (holes) are transformed into spin polarons and spinless bipolarons. From the calculated density of states, it was found that spin-polarized injection is possible when the Fermi level of CMR lies below the bipolaron level of the polymer. However, if the Fermi level of CMR lies above the bipolaron level of the polymer, the injected electrons (holes) form bipolarons, which have no spin, and there is no spin distribution in the polymer spacer. Later in 2006, we investigated the dynamic process of charge injection in a conjugated polymer chain contacted with a metal electrode in the framework of a nonadiabatic approach.[63] It was found that the injected charges form localized wave packets due to the strong electron–lattice interactions in the conjugated polymer. A wave packet may contain any quantity of charges up to two electronic units, with the quantity depending on the injection conditions. For a spin degenerate system, a wave packet has no spin. Especially, when the wave packet carries one electronic unit, it has no spin although the lattice distortion of the

wave packet has the characteristic of a polaron. A wave packet cannot contain more than two electronic units because of the Pauli exclusion. However, for a spin-nondegenerate system, such as a CMR/polymer system, the spin-polarized electrons are injected from the half-metal CMR. In this case, the injected charges will form a spin-polarized wave packet. A polaron with one electron and 1/2 spin may be obtained.

Figure 4 gives the evolution of the injected charges in an organic layer in contact with a ferromagnetic metal. As the whole system is spin-nondegenerate, there is a net spin distribution. With the evolution, the amplitude of the spin decreases. We define the spin polarization as

$$P = \sum_{n\in\text{polymer}} \left|\rho_{n,\,s=\uparrow} - \rho_{n,\,s=\downarrow}\right| \Big/ \sum_{n\in\text{polymer}} \left|\rho_{n,\,s=\uparrow} + \rho_{n,\,s=\downarrow}\right|. \quad (4)$$

The time dependences of the spin polarization under different electrical fields are shown in Fig. 5. It is found that the spin polarization is the largest at the interface and decays oscillatorily into the organic layer.

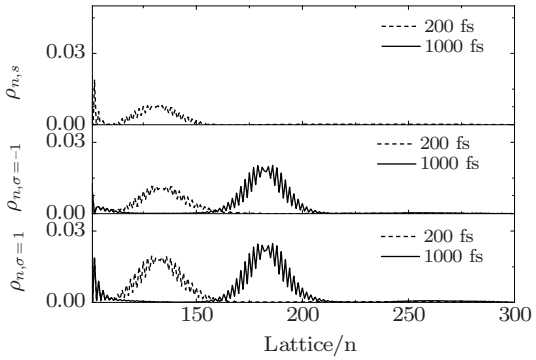


Fig. 4. Distribution of the spin-up, spin-down, and net spin density in different time. The bias is $V = 0.85$ V and the electric field is $E = 0.5$ mV/nm.

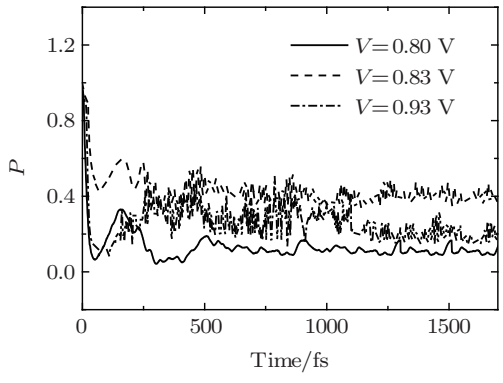


Fig. 5. Time dependences of the spin polarization under different biases.

With the Green function theory, Zwolak *et al.* calculated spin-dependent transport in short DNA molecules sandwiched between ferromagnetic contacts using a tight-binding model.[64] They showed that a DNA spin valve can be realized with MR values as high as 26% for Ni and 16% for Fe contacts, as shown in Fig. 6. The spin-dependent transport can broaden the possible applications of DNA as a component in molecular electronics and shed new light on the transport properties of this important biological molecule.

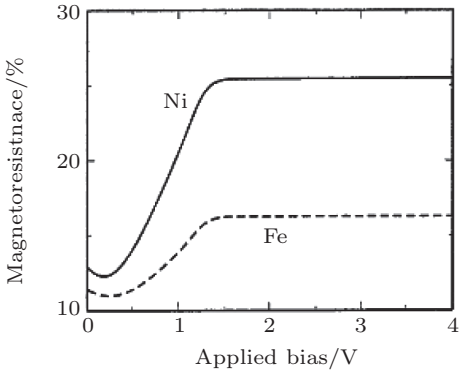


Fig. 6. MR as a function of bias for both Ni and Fe contacts at room temperature.[64]

4.1.2. Spin polarization

Organic ferromagnets are also used to study the spin transport. For a metal/poly-BIPO/metal device, an extended SSH + Heisenberg model[65] was adopted to describe the ferromagnetic poly-BIPO molecule, which contains the electron–lattice coupling and the spin correlation between π electrons and the residual spins of radical R's. The spin-dependent Landauer–Büttiker formula[47] was employed to calculate the current–voltage (I–V) characteristics through the device.

The calculated I–V curves are shown in Fig. 7(a), where the spin-up and spin-down curves are calculated separately. The total current is given by $J = J_\uparrow + J_\downarrow$. It is found that the spin up tunnel and the spin-down one will be opened at different lifting voltages. Defining the spin polarization of the current as Eq. (1), we obtain that the current is spin-polarized and oscillates with the applied voltage, as shown in Fig. 7(b). It is especially noteworthy that, when $V > 0.5$ V, a spin polarization near 100% is obtained, which means that, in this region of the bias, only one spin tunnel of the current is opened.

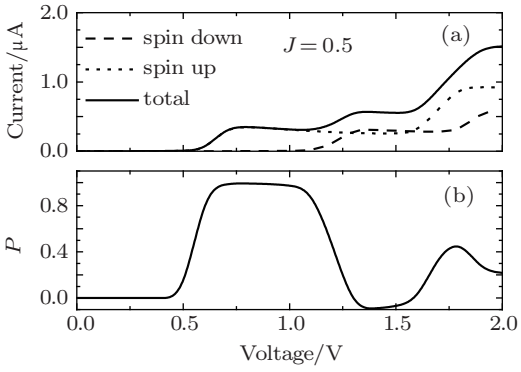


Fig. 7. (a) The calculated I–V characteristics of a model device. (b) Spin polarization of the current as a function of the bias.

The behavior of the spin polarization is explained in the following. Due to the spin correlation between π electrons

and the residual spins, the conjugated conducting π orbitals in the main chain are spin split. The LUMO of the spin up levels is closer to the Fermi level of the electrodes than that of the spin down ones. Applying a bias, the spin up channel will be opened first, which permits a spin-polarized current. With increasing bias, the LUMO of the spin down levels begins to conduct current. Thus the total current increases while the spin polarization decreases. As more and more orbitals begin to conduct current, the spin polarization oscillates.

The most interesting feature is that a 100% spin polarization may be obtained in some regions of the bias. Due to the strong electron–lattice interaction in such organic molecules, there is a large Pereils gap between the LUMO and HOMO levels for spin up or down electrons. When the bias increases to 0.5 V under the present parameters, only the spin up channel (LUMO) is opened while the spin down one is blocked by the large energy gap. Therefore, the current is contributed only by the spin up tunnel, which results in a 100% spin polarization. For a typical ferromagnetic metal, there is no gap. Thus, it is difficult to get a large spin-polarized current. Our investigation suggests the possible application of an organic ferromagnet in a spin filter device with no external field modulation.

The spin polarization in a ferromagnetic molecule device may be changed by photoexcitation. In the organic ferromagnet poly-BIPO, the existence of a spin-excited state means that the ferromagnetic order of radical spins is destroyed, owing to the spin flipping, which induces a high energy state in the magnetic molecule. As the radical spins are correlated with the π-electrons in the main chain, it is expected that the spin-excited state will affect the transport of π-electrons along the main chain. We calculated the transport properties of the device and found the total current suppression and spin polarization modulation effect in multiple spin-excited states.

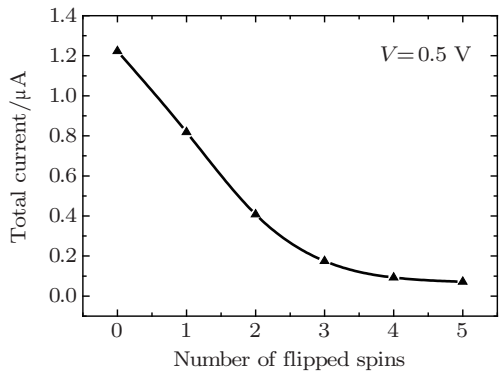


Fig. 8. The dependence of total current on the number of flipped radical spins at a certain bias.

Figure 8 shows that the total current decreases rapidly until it disappears as the number of excited radical spins decreases, at a fixed bias of $V = 0.5$ V. The total current suppression effect has also been found experimentally in a single molecular magnet. This can be explained by the transmission of the LUMO of the spin up electron in the conducting region. The LUMO, which takes part in conducting, moves out of the bias window gradually with increasing number of excited radical spins. Meanwhile, the transmission peak decreases gradually because of the localization of the wave function. By utilizing the total current suppression effect, we predicted that, by modulating the number of excited radical spins, the organic ferromagnetic device can realize controllable charge transport. In addition, when a ferromagnetic molecule is excited from the ground state to the highest spin-excited state, a conductance switch functionality can be implemented.

4.1.3. Spin-current rectification

The molecular rectifier, which may realize an asymmetric I–V characteristic at the molecular level, will play a crucial role in the electronic logic circuits of future nanoscale electronics. Recent experimental and theoretical researches have proved that an asymmetric molecule can act as an intrinsic charge-current rectifier.[1,2] Although molecular spintronics has attracted much interest, such as spin injection into organic materials,[3] MR in molecular tunnel junctions,[66] and spin filtering in magnetic molecules,[40] the design of a functional device based on the electron spin is still an important topic needing more research.

The concept of spin-current rectification (SCR) has been proposed,[67] which means that the spin transport is not symmetric under an external driving field. An SCR is more complex to describe than the charge-current rectification (CCR) because a spin current has both amplitude and polarization. One kind of SCR is that in which only the spin-current amplitude is asymmetric and its spin-polarized orientation remains unchanged when the bias is reversed. This kind of SCR is analogous to the normal CCR, and we call it the parallel spin-current rectification (PSCR). Another kind of SCR is that in which the spin-polarized orientation of the spin current flips when the bias is reversed. In this case, the amplitude of the spin current may be either symmetric or asymmetric, and we call this kind of SCR the antiparallel spin-current rectification (ASCR).

We designed an organic spin diode to obtain the SCR, which is based on an organic magnetic co-oligomer or an organic magnetic/nonmagnetic hetero-junction structure. The electrodes are semi-infinite one-dimensional metallic chains. The spacer is an organic copolymer composed of ferromagnetic molecules (such as poly-BIPO) and the right nonmagnetic one (such as polyacetylene). This kind of copolymer is spatially asymmetric in the spin and charge degrees of freedom. By extending the Landauer–Büttiker formula, both the charge current and the spin current through the device are calculated.

Both PSCR and ASCR are realized by adjusting the relative location of the Fermi level of the electrodes. In Fig. 9, the Fermi level of the electrodes is taken as $E_F = 0$. The results show that there is no CCR in this case. But the SCR appears, that is, by reversing the applied bias. Although the spin-current magnitude remains symmetric, the spin orientation of the current is changed from spin down to spin up. We call this kind of SCR ASCR, as defined above. The intrinsic mechanism is an asymmetric shift of the molecular orbitals in the spin degree of freedom induced by the bias. Under a positive bias, the spin-down HOMO enters the conducting bias window first and contributes to the current. Vice versa, the spin-up LUMO will conduct current first when a negative bias is applied.

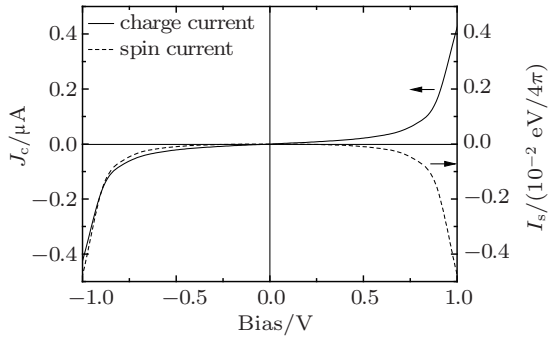


Fig. 9. Calculated charge current and spin current as a function of the bias voltage with $E_F = 0$. Here $J_c = J_\uparrow + J_\downarrow$ and $J_s = \frac{\hbar}{2e}(J_\uparrow - J_\downarrow)$.

A more complex case is that both CCR ($J_c(-V) \neq -J_c(V)$) and SCR ($J_s(-V) \neq -J_s(V)$) appear, which implies the realization of an active device that combines electric logic and magnetic memory functions. It requires asymmetries in both the charge and the spin degrees of freedom. This condition can be satisfied by adjusting the relative Fermi level of the electrodes to that of the molecule. One result at $E_F = 0.3$ eV is shown in Fig. 10. It is found that both CCR and SCR appear when the applied bias is reversed. The spin orientation of the spin current remains unchanged in spite of the asymmetric amplitude. Thus, the PSCR is realized in the device. A deeper understanding can be achieved by a molecular orbital analysis.

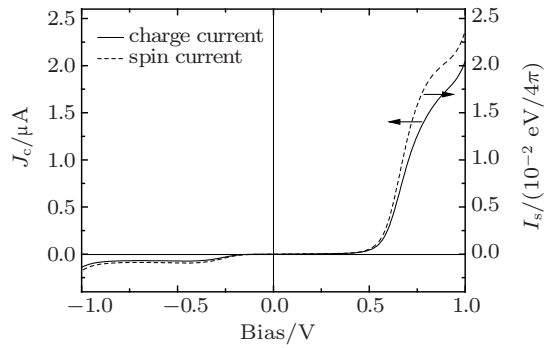


Fig. 10. Calculated charge current and spin current versus bias with $E_F = 0.3$ eV.

4.1.4. Spin precession in organic polymers

To understand the microscopic mechanism of organic spintronics, one needs to study the spin precession in OSCs. The spin-related interactions in OSCs include the spin–orbit coupling and other possible spin-related interactions. Usually, the spin–orbit coupling in organic polymers is considered to be weak, and most of the present work neglects its effect on the spin transport in organic devices. However, it has also been predicted that the spin–orbit coupling may be effective in some OSCs with special structures.[68,69] Moreover, by applying a gate voltage, it is hoped that some effects of the Rashba spin–orbit coupling will be observed, especially for the particle-like polarons. Therefore, it is necessary to investigate the spin dynamics of a polaron in an OSC.

The Hamiltonian is $H = H_0 + H_{so}$, where

$$H_0 = -\sum_{n,s} t_{n,n+1}\left(e^{-i\gamma A} C^+_{n+1,s} C_{n,s} + \text{h.c.}\right) + \frac{1}{2}K\sum_n (u_{n+1}-u_n)^2 + \frac{1}{2}M\sum_n \dot{u}_n^2, \quad (5)$$

$$H_{so} = -t_{so}\sum_n \left[e^{-i\gamma A}\left(C^+_{n+1,\uparrow} C_{n,\downarrow} - C^+_{n+1,\downarrow} C_{n,\uparrow}\right) + \text{h.c.}\right]. \quad (6)$$

Here, $t_{n,n+1} = t_0 - \alpha(u_{n+1} - u_n)$ is the electron transfer between sites n and $n+1$ adjusted by the site derivation u_n from its equilibrium position, α is the electron–phonon coupling constant, $C^+_{n,s}$ ($C_{n,s}$) is the electron creation (annihilation) operator on site n with spin s. Vector potential $A = A(t)$ becomes scalar along the molecule chain direction and is related to the external parallel electric field through $E(t) = -\partial_t A(t)$. Coefficient γ in the exponent is defined as $ea/\hbar$, with e and a being the electron charge and the lattice constant, respectively. The H_{so} describes the spin–orbit coupling in the OSC with intensity t_{so},[70] which is effectively produced by a gate electric field (Rashba electric field) $\boldsymbol{E} = E_{so}\boldsymbol{z}$ perpendicular to the chain. A one-dimensional polymer chain along the x axis with a periodic boundary condition is considered.

We have theoretically investigated the spin dynamics of a polaron in a one-dimensional organic polymer chain using a nonadiabatic evolution method. Suppose that a spin-up electron ($+\hbar/2$ along the z axis) is injected into the polymer chain. A weak electric field is applied along the chain to drive the charged polaron along the chain. The evolution of the spin of the polaron is shown in Fig. 11. It is found that the polaron spin $\langle s_z \rangle$ presents a cosinoidal-like oscillation, which is the spin precession caused by the spin–orbit coupling. As a polaron is a localized state, it is found that the spin procession takes place only within the polaron level (or intralevel), which is different from the case of an extended state in a rigid semiconductor, wherein the spin procession takes place among all the conduction levels (or interlevel).[71] The spin precession period of a polaron is determined by the strength of the spin–orbit coupling. Therefore, we can control the spin transport in

an organic polymer by applying an external Rashba effective field.[72]

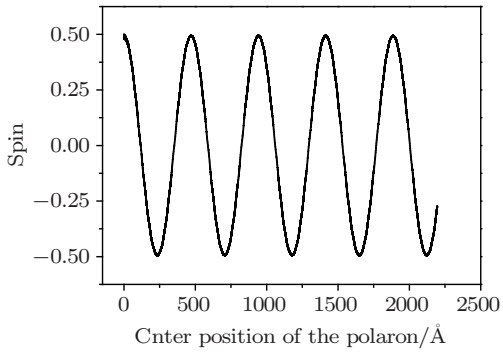


Fig. 11. Precession period length for different strengths of spin–orbit coupling in the organic polymers.

4.1.5. Spin diffusion

Spin diffusion theory has been used to describe the spin-polarized current in spin injection into inorganic semiconductors based on the two-current model.[73–82] It is hoped that this theory can be adapted to the study of spin dependent injection and transport in OSCs. Of course, the characteristics of OSCs should be addressed. For example, the carriers in OSCs are localized polarons and bipolarons, of which only the polarons carry spin. Ruden and Smith have presented a theoretical model to describe the electrical spin injection from a ferromagnetic contact into a conjugated organic material.[83] They have found that a quasi-equilibration between the conjugated organic material and the metallic contact must be suppressed to achieve effective spin injection. The spin-dependent barrier to electrical injection may be due either to tunneling through the depletion region of a large Schottky barrier or to tunneling through a thin, insulating, interface layer. The thermoionic emission, surface recombination, tunneling through the barrier, and drift-diffusion were then considered. Yu *et al.* described the spin transport across a polymer sandwiched between magnetic contacts with arbitrary magnetization directions. They found that even a weak magnetic field can significantly modify the spin transport in polymers through spin precession. It was shown that the interplay of spin drift due to electric field and spin precession can lead to damped oscillating MR as the magnetic field increases.[84,85]

Our group also studied the spin-polarized injection and transport in organic devices with the classical spin diffusion theory, which was based on the coexistence of polarons and bipolarons in one OSC.[86,87] These quasi-particles have special charge–spin relations, as mentioned above. Due to the effects of temperature, pressure, and external field, polarons and bipolarons in OSCs can transform into each other. Two spin polarons can annihilate into one spinless bipolaron, while one spinless bipolaron can decouple into two spin polarons.[88] Therefore, in an organic device, three carrier channels should exist in the transport layer: spin-up polaron, spin-down polaron, and spinless bipolaron channels.[89,90] If one assumes that no strong spin-flip scattering occurs at the interfacial layer between the ferromagnetic and the organic materials, and (for simplicity) no space charge exists, the current through the device can be supposed to obey the Ohm's law. Then, from the spin diffusion theory and the Ohm's law, one can obtain the interfacial current spin polarization by adding the corresponding interfacial relation, giving

$$P_0 = \gamma\cdot\beta_0\cdot\frac{\lambda_{\rm FM}}{\sigma_{\rm FM}}\cdot\frac{\sigma}{\lambda_{\rm p}}\cdot\frac{1+\frac{1}{4\beta_0}\cdot\frac{\sigma_{\rm FM}}{\lambda_{\rm FM}}\cdot\left(\frac{1}{G_\downarrow}-\frac{1}{G_\uparrow}\right)\cdot\left(1-\beta_0^2\right)}{\left(\gamma\cdot\frac{\lambda_{\rm FM}}{\sigma_{\rm FM}}\cdot\frac{\sigma}{\lambda_{\rm p}}+1\right)-\beta_0^2+\frac{\gamma}{4}\cdot\frac{\sigma}{\lambda_{\rm p}}\cdot\left(\frac{1}{G_\downarrow}+\frac{1}{G_\uparrow}\right)\cdot\left(1-\beta_0^2\right)}. \tag{7}$$

where the polaron proportion in the OSC is defined as $\gamma = n_{\rm p}/(n_{\rm p}+n_{\rm bp})$, $n_{\rm p}$ and $n_{\rm bp}$ are the densities of the polarons and the bipolarons, respectively. The dependence of current spin polarization P_0 on the polaron proportion γ is shown in Fig. 12.

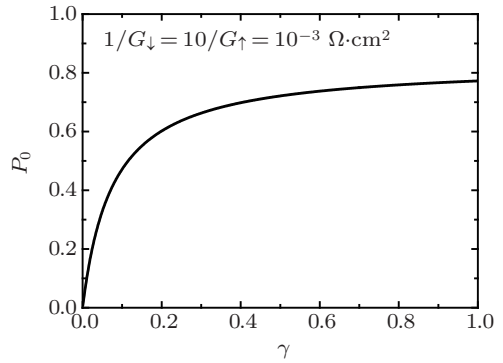


Fig. 12. Dependence of current spin polarization P_0 on the polaron proportion γ.

The maximum spin polarization is obtained at $\gamma = 1$ because all of the carriers are spin polarons in this case. Here, the result is similar to the case in the inorganic semiconductors with electrons (or holes). But at $\gamma = 0$, there is no spin polarization because in this case all the carriers in the organic layer are spinless bipolarons. In addition, it is also found that significant spin polarization appears as soon as polarons come into existence. For example, even if only 20% of all carriers are polarons, the spin polarization will be about 90% of the value attainable with only polarons and no bipolarons. Therefore, the spinless bipolarons are not very important even in the organic materials where they exist, such as highly conjugated

polymers. The spin polarons are effective carriers of a spin-polarized current, even if they constitute only a fraction of all carriers.

Based on the drift-diffusion equations, we further investigated spin injection and transport from a ferromagnetic contact to an OSC. Here a polaron–polaron interaction model is suggested to understand the polaron–bipolaron transition[91]

$$s_{\uparrow(\downarrow)} = -kn_{\uparrow}n_{\downarrow} + bN, \tag{8a}$$

$$s_N = kn_{\uparrow}n_{\downarrow} - bN, \tag{8b}$$

where $n_{\uparrow(\downarrow)}$ is the density of spin-up (spin-down) polarons and N is the density of bipolarons. The first term on the right of Eq. (8a) describes the probability that a spin-up (-down) polaron encounters a spin-down (-up) one to annihilate into a spinless bipolaron. The second term describes the reversed process: a bipolaron decomposing into a spin-up polaron and a spin-down polaron. Parameters k and b express the transition strength and are both dependent on the temperature. We define the spin polarization $P = (n_{\uparrow} - n_{\downarrow})/(n_{\uparrow} + n_{\downarrow})$ to analyze the spin characteristic of the injected charges in the OSC. Note that another definition for the spin polarization, $P = (n_{\uparrow} - n_{\downarrow})/(n_{\uparrow} + n_{\downarrow} + n_{\mathrm{bp}})$, may be adopted in the case of polaron and bipolaron coexistence.

Unlike the case in an inorganic semiconductor, two factors affect the relaxation of spin in OSCs: the spin-flip effect and the transition between polarons and bipolarons. By supposing that the injected electrons from the ferromagnetic contact are fully spin-polarized polarons when they enter an OSC, we obtain the evolutions of bipolarons and polarons during their transport in the OSC. The appearance of bipolarons decreases the density of the spin carriers (polarons) and thus affects the spin polarization of the system. It is found that the densities of polarons and bipolarons will reach a dynamic equilibrium during their transport in the OSC. Then, the spin polarization is dominated mainly by the spin-flipping of polarons. We also find that a large spin diffusion length in the OSC can be obtained through a large mobility or a long spin-flip time of spin polarons.

Figure 13 shows that, if there are no bipolarons during the transport, the spin polarization decays exponentially, which is similar to the case in a normal inorganic semiconductor injection if we replace electrons in an inorganic semiconductor with spin polarons in an OSC. However, bipolarons change the distribution of spin polarons, affecting the spin polarization. It is interesting that the appearance of bipolarons increases the spin polarization.

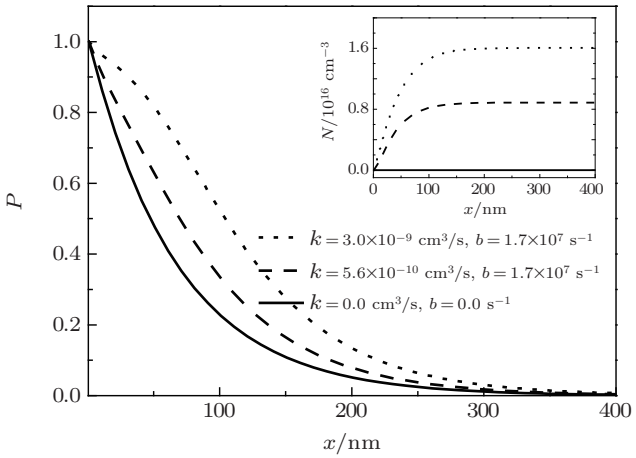


Fig. 13. Distribution of spin polarization P with different bipolaron density. The variation in bipolaron density, shown in the inset, is obtained by adjusting parameters k and b.[91]

4.2. Organic magnetic field effect

With the explosive investigation of spin transport in organic devices, another phenomenon, the organic magnetic field effect (OMFE), has aroused curiosity.[92] At room temperature, electrical and optical properties of nonmagnetic OSCs respond significantly to a low magnetic field (in the scale of mT), even in the absence of magnetic contacts - the blanket term for these responses is OMFE.[93,94] Two aspects of OMFE, OMAR and organic magnetoconductance (OMC, the inverse of OMAR), show universal line shapes that can be fitted by empirical Lorentzian $B^2/(B^2 + B_0^2)$, non-Lorentzian $[B/(|B| + B_0)]^2$, or their combination.[95,96] Some can also be fitted by power law B^n, $f_1/B^2 + f_2/B^4$, or $d_1B^2 + d_2B^4$.[97,98] OMAR values around 0%–15% have been observed in a number of OSCs. In some cases, an MR value over 300% has also been observed.[99] In addition, both positive and negative OMAR have been reported, changing between negative and positive depending on the voltage, temperature, and layer thickness.[95,100–103]

We will next describe the experimental and theoretical researches into OMAR and then present our own contribution in this area.

4.2.1. Experiments on OMFE

In 2005, Mermer *et al.* were the first to report the OMAR effect in polyfluorene (PFO) sandwich devices. The MR value reaches up to 10% at a magnetic field of 10 mT at room temperature.[94,95]

A schematic drawing of the device and the experiment on OMAR is shown in Fig. 14. The samples were mounted on the cold finger of a closed-cycle helium cryostat located between the poles of an electromagnet. MR, which is defined as $\mathrm{MR} = [R(B) - R(0)]/R(0)$, was obtained by measuring the current at a constant driving voltage for different magnetic fields B.

Figure 15 shows MR curves in an ITO/PFO($\approx$ 60 nm)/Ca

device. They found that the MR is negative under a low applied voltage, while it becomes positive at high applied voltages.

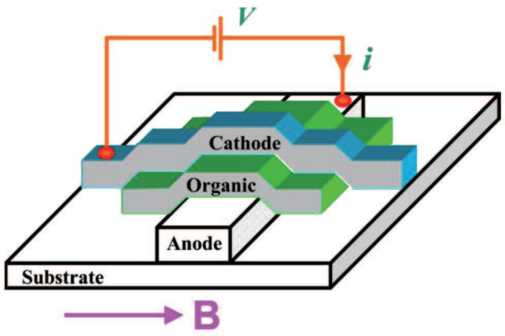


Fig. 14. Schematic drawing of the device and the MR experiment.[95]

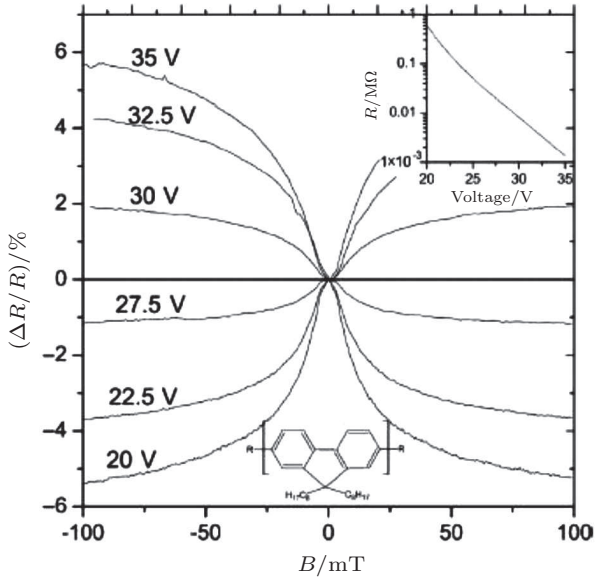


Fig. 15. MR measured at 200 K in an indium-tin-oxide (ITO)/PFO(≈ 60 nm)/Ca device at different voltages. Inset shows device resistance as a function of applied voltage.[95]

An apparent OMAR effect was also found in organic devices fabricated with small molecules. The measured OMAR traces in Alq_3 devices are shown in Fig. 16. It was further found that the OMAR behavior is independent of the angle between the film plane and the applied magnetic field.[104]

Nguyen *et al.* described the magneto-electroluminescence response in organic light-emitting diodes, which is based on π-conjugated polymers made of protonated and deuterated poly(2,5-dioctyloxy-pphenylenevinylene) (DOO-PPV) (the latter has a weaker hyperfine interaction (HFI)).[105] It was found that the device based on the D-polymers shows significantly narrower OMFE responses, as shown in Fig. 17. Also, as shown in Fig. 18, they found that the magneto-electroluminescence (MEL) response changes sign on a small magnetic-field scale. This seems to indicate that the HFI may be vital for the performance of OMFE.

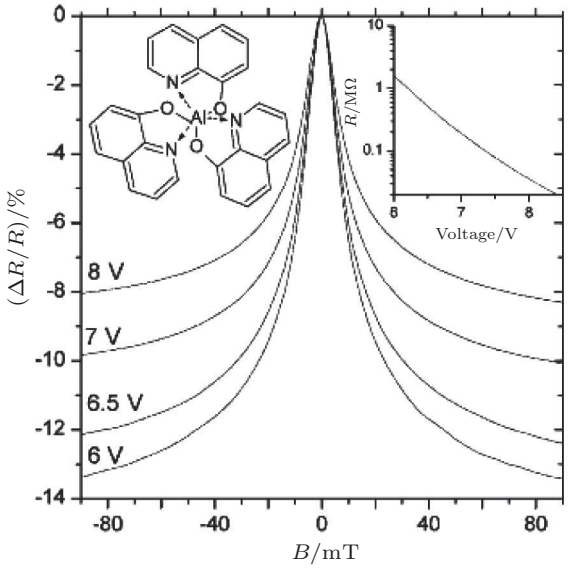


Fig. 16. MR measured at room temperature in an ITO (30 nm)/poly(3, 4-ethylenedioxythiophene)poly(styrenesulfonate) (PEDOT) (≈ 100 nm)/Alq_3 (≈ 50 nm)/Ca (≈ 50 nm including capping layer) device at different voltages. The inset shows device resistance as a function of applied voltage.[104]

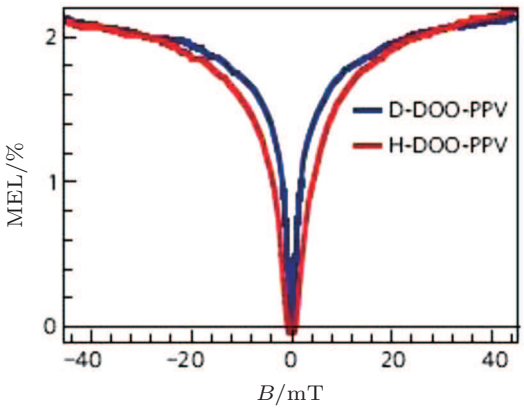


Fig. 17. Isotope dependence of the MEL response in OLEDs based on DOO-PPV polymers, plotted on a large magnetic-field scale.[105]

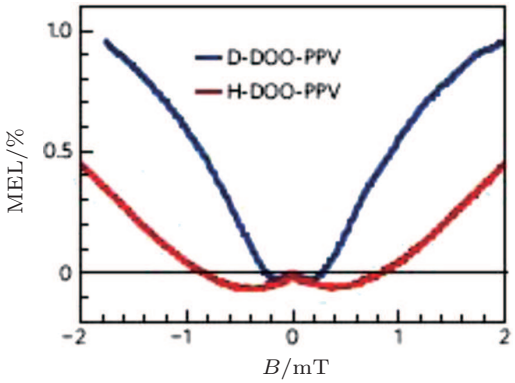


Fig. 18. Isotope dependence of the MEL response in OLEDs based on DOO-PPV polymers, plotted on a small magnetic-field scale.[105]

Zhang *et al.* also presented the ultra-small field magnetoconductance (MC) induced effects in the super yellow poly(phenylenevinylene) SY-PPV:phenyl-C61-butyric acid methyl ester (PCBM) blends to clarify the role of competition between dissociation and spin-mixing to influence the

MC response. The width of the ultra-small field-induced MC was found to be broadened with increasing PCBM concentration in the blend devices.[106]

As the organic devices exhibit highly nonlinear current-voltage characteristics, OMAR is tightly related to the driving voltage. Desai *et al*. reported that, at a driving voltage around the open-circuit voltage in an Alq_3 light-emitting diode, where the current through the device is very small, an MR value as large as 300% can be observed at room temperature.[99] Recently, Mahato *et al*. predicted an exceptionally large (> 2000%) OMAR effect in one-dimensional systems formed by molecular wires embedded in a zeolite host crystal. This ultrahigh MR effect was attributed to the spin blockade in the one-dimensional electron transport.[107]

4.2.2. Theory of OMFE

There are a proliferation of models for spin-dependent electronic processes in OSCs. For OMFE or OMAR, it seems that new observations are explained with new models rather than serving to scrutinize existing models.[108] Even so, the theoretical exploration in the past ten years has provided vast information to help understand the strange effects in OSCs. The spin related interaction itself is extremely complex, especially in asymmetrically structured OSCs. As mentioned above, when a magnetic field is applied, the interactions include not only the spin-Zeeman interaction but also the charge-Lorentzian interaction; the hydrogen nuclear spin hyperfine interaction may also be involved. For example, Yu *et al*. presented a systematic study of HFI and its role in organic spintronic applications.[109] Up to now, three mechanisms have been suggested for OMFE: polaron pair mechanism, bipolaron mechanism, and exciton quenching mechanism. The polaron pair model focuses on the dissociation- and recombination-related process. The bipolaron model focuses on the mobility-related process. The exciton model focuses on exciton quenching due to collisions. All these mechanisms may be considered via either the spin-Zeeman interaction or the charge-Lorentzian interaction, which results in OMFE.

From the basic charge-mobility relationship $J = nev$, we know that the current J is dependent upon not only the carrier density n, but also the carrier velocity v. For a weak field and not-too-large MC (or MR), we have

$$\begin{aligned} \mathrm{MC} &\doteq \frac{n(B)-n(0)}{n(0)} + \frac{v(B)-v(0)}{v(0)} \\ &= \mathrm{MC}(n,B) + \mathrm{MC}(v,B), \end{aligned} \tag{9}$$

where $\mathrm{MC}(n,B)$ and $\mathrm{MC}(v,B)$ are the responses of density and mobility of magnetic field, respectively. The experimental investigation seems to reveal that both the carrier density and the mobility μ ($\mu = v/E$ with E being the electric field strength) will be affected by the magnetic field. For example, by using electroluminescence spectroscopy and charge-induced absorption spectroscopy techniques, Nguyen *et al.* measured the respective dependencies of singlet exciton, triplet exciton, and polaron densities on the applied magnetic field.[110] They found that all the densities increased with increasing magnetic field. However, Veeraraghavan *et al.* performed a magnetoresistance measurement in PFO devices and showed that the magnetic field effect acted on the carrier mobility rather than the carrier density.[111] In addition, Ding *et al.* recently found that MEL has a close relationship with the carrier mobility during their investigation of the magnetic field effect in organic light emitting devices with an NPB:Alq_3 mixed emission layer.[112]

Polaron pair model In a bipolar organic device, injected electrons and holes may form intramolecular excitons and intermolecular polaron pairs. It is now believed that the intramolecular excitons are usually in singlet states, while the intermolecular polaron pairs are in ether singlet or triplet states. The singlet/triplet ratio is about 1:3 if we do not consider any spin related interaction effect. The intersystem crossing between the singlet and the triplet pairs will take place when a magnetic field is applied. This will result in the different contribution of singlet and triplet polaron pairs for dissociation or recombination. Therefore, the change in the singlet/triplet ratio in polaron pairs by the external magnetic field would change the emission or the current (photocurrent or dark current). In other words, as the intersystem crossing is changed by the external magnetic field, the singlet/triplet polaron pair ratio is changed and then the magnetic responses occur.[113]

Bipolaron model In an unipolar organic device, only one kind of charge (electrons or holes) is injected. In this case, the bipolaron model was proposed, which is based on the transition between polarons and bipolarons. When the magnetic field is absent, the spin singlet polaron pairs dominate in OSCs. When the magnetic field is applied, the proportion of triplet polaron pairs increases because of the interruption to the spin-magnetic field interaction. The mobility of the system decreases due to the low mobility of the triplet pairs compared to that of the singlet ones. This leads to a decrease in current and generates a positive MR. When including the long range Coulomb repulsion, a negative sign or a negative MR can be obtained. The long range Coulomb repulsion is believed to enhance the bipolaron formation. The number of bipolarons is decreased by applying a magnetic field, but the number of free charge carriers is increased, which generates a negative OMAR.[114]

Exciton quenching model The exciton quenching model is based on the exciton–polaron reaction[115] and the exciton–exciton annihilation.[116] Both focus on the triplet exciton quenching process due to the long lifetime of the triplet excitons. A polaron may meet a triplet exciton in moving. Their

interaction will result in the creation of a singlet exciton. It is found that the rate constant of the triplet–polaron reaction process can be changed by the external magnetic field. The triplet–triplet annihilation process is that two triplet excitons collide with each other and eventually annihilate into a singlet exciton. The negative magnetic field effect for delayed fluorescence has been observed in organic molecular crystals, motivating the proposal that a magnetic field can modulate the rate constant of the triplet–triplet annihilation reaction.

From the rate equation, we may understand the OMFE in a simple manner. By introducing the transition rate $\gamma_{\rm ap}$ to describe the hopping from a spin-parallel polaron pair to a spin-antiparallel one and $\gamma'_{\rm ap}$ for the reverse process, we write the dynamic equations of these carriers as

$$\frac{{\rm d}n_{\rm pp}}{{\rm d}t} = -\gamma_{\rm ap} n_{\rm pp} + \gamma'_{\rm ap} n_{\rm ap}, \tag{10a}$$

$$\frac{{\rm d}n_{\rm ap}}{{\rm d}t} = +\gamma_{\rm ap} n_{\rm pp} - \gamma'_{\rm ap} n_{\rm ap} + k n_{\rm bp} - b n_{\rm ap}, \tag{10b}$$

$$\frac{{\rm d}n_{\rm bp}}{{\rm d}t} = -k n_{\rm bp} + b n_{\rm ap}, \tag{10c}$$

where $n_{\rm pp}$ ($n_{\rm ap}$) is the spin-parallel (-antiparallel) polaron pair density, $n_{\rm p}$=2($n_{\rm pp}+n_{\rm ap}$), $n_{\rm bp}$ is the density of bipolarons, and $-\gamma_{\rm ap} n_{\rm pp}$ ($+\gamma'_{\rm ap} n_{\rm ap}$) represents the decrease (increase) of the spin-parallel pair density due to spin-mixing. Parameter b describes the local recombination rate for pairs of polarons of opposite spins forming bipolarons, while k describes the reverse process.

To obtain the transition rate, we represent the polaron spin-Zeeman effect and the hyperfine interaction as

$$\hat{H} = g\mu_{\rm B} B \hat{S}_z + a\hat{\boldsymbol{I}} \cdot \hat{\boldsymbol{S}}, \tag{11}$$

where $\mu_{\rm B}$ is the Bohr magneton, $\hat{\boldsymbol{S}}$ and $\hat{\boldsymbol{I}}$ the polaron and the hydrogen nuclei spin, respectively, g is the g factor, and a denotes the strength of the hyperfine interaction. The hyperfine interaction is treated within quantum mechanics. We give the transition rate between a spin-parallel polaron pair and a spin antiparallel one by considering all possible configurations of the hydrogen nuclei spin states. By considering that the carrier density variation is the main reason for the MC effect, the MC is obtained as

$$\mathrm{MC} = \mathrm{MC}_\infty \frac{\omega^4}{\omega^4 + 2\beta a^2 \omega^2 + \beta a^4},$$

where $\mathrm{MC}_\infty = \frac{2(1-\alpha)k/b}{(\alpha+2k/b)(7+16k/b)}$ is the saturated MC value, $\alpha = v_{\rm bp}/v_{\rm p}$ is the velocity ratio between polaron and bipolaron, $\beta = 1 + \frac{1}{16k/b+7}$, and ω=$g\mu_{\rm B}B$. It is found that the MC behavior is tightly related to the magnetic field and the hyperfine interaction. As $\beta \approx 1$, when the magnetic field is stronger than the hyperfine effective field, $B \gg B_{\rm hf}$ ($\omega \gg a$), we have

$$\mathrm{MC} = \mathrm{MC}_\infty \frac{\omega^2}{\omega^2 + 2\beta a^2} = \mathrm{MC}_\infty \frac{B^2}{B^2 + 2\beta B_{\rm hf}^2},$$

which is a fully saturated trace and is well fitted to the Lorentzian form to explain the experimental data. However, if the external magnetic field is small, $B < B_{\rm hf}$, or the values of the magnetic field and the hyperfine field are close to each other, the MC will deviate from the Lorentzian function. Especially, the line shape of MC(n,B) is closely related to the hyperfine interaction, which indicates the importance of the hyperfine interaction in OMC. It is also obtained that the branching rate of the bipolarons plays a significant role in the OMC behavior.[117] As shown in Fig. 19, in the case of a small branching rate of bipolarons, the MC increases with the rate; while in the case of a large branching rate, the MC decreases with the rate. It has been reported that, in small molecular device PEDOT/Alq_3/Au,[104] the MC increases with the applied voltage or injected carrier density (as shown in the inset of Fig. 19, left). Combining the above analyses, we speculate that bipolarons are the minority in Alq_3. But in polymer device ITO/PFO/Au,[94] it was reported that the MC decreases with the applied voltage (as shown in the inset of Fig. 19, right). As polarons extend to be confined into bipolarons in polymers, we speculate that bipolarons are the majority in PFO.

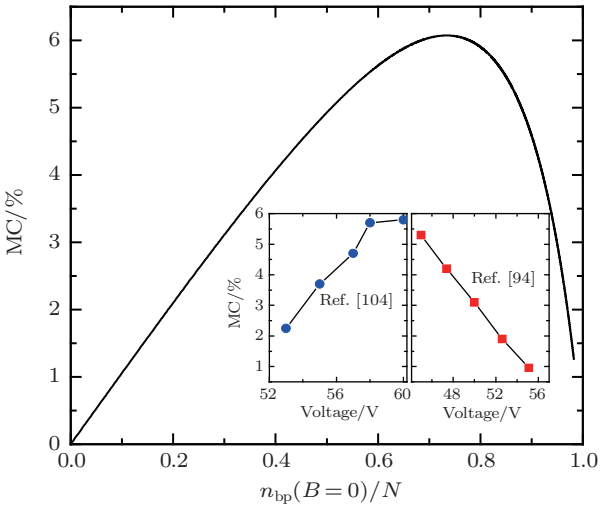


Fig. 19. MC as a function of bipolaron ratio, where external magnetic field B = 100 mT and α = 0.15. The insets show MC as a function of the applied voltage.

Based on a quantum quasi-band model, we have investigated the polaron dynamics under a magnetic field.[118] We consider theoretically the effect of the magnetic field on the carrier (polaron) velocity. To describe the moving of a polaron, we adopt the tight-binding model suggested by Troisi and Orlandi.[31] The Hamiltonian reads

$$H_{\rm TO} = \sum_{j,s} [-\tau + \alpha(u_{j+1} - u_j)](C^+_{j+1,s} C_{j,s} + C^+_{j,s} C_{j+1,s}) + \sum_j \frac{1}{2} m\dot{u}_j^2 + \sum_j \frac{1}{2} K u_j^2, \tag{12}$$

where the notations have the same meaning as those in Ref. [31].

The effects of the magnetic field and the hyperfine interaction are considered as in Eq. (12). When an external magnetic field is absent, the expectation of the nuclei spin vector $\boldsymbol{B}_{\mathrm{hyp},j} = \langle \hat{\boldsymbol{I}}_{\mathrm{hyp},j} \rangle$ is random both in value and orientation. When the magnetic field is applied, we suppose that the distribution of the expectation $\boldsymbol{B}_{\mathrm{hyp},j}$ is governed by the Boltzmann distribution, i.e., $f(\varepsilon) \propto \mathrm{e}^{-\varepsilon/k_{\mathrm{B}}T}$. Here $\varepsilon = -g_{\mathrm{I}}\mu_{\mathrm{N}}B_{\mathrm{hyp}} \cdot B\cos\theta$, and θ is the angle between $\boldsymbol{B}$ and $\boldsymbol{B}_{\mathrm{hyp}}$.

It is found that, when an external magnetic field is applied, the motion of the spin polaron will be disturbed due to the spin-related interaction with the magnetic field and the hydrogen nuclear spins. Figure 20 shows the dependence of MR on the applied magnetic field at different hyperfine intensities. The theoretical calculations are quite consistent with the experimental data. It is also found that the hyperfine interaction is a dominating factor for the appearance of the OMAR effect in a non-magnetic OSC. As shown in the figure, the MR value decreases with increasing hyperfine intensity or deuteration, which agrees with the experimental conclusion. In addition, by changing the e–ph coupling α, we find that the OMAR will change correspondingly. For example, fixing the external magnetic field to $B = 80$ mT, the MR increases from 0.38% at $\alpha = 140$ meV/Å with a polaron width of 34.4 Å to 1.93% at $\alpha = 180$ meV/Å with a polaron width of 12.4 Å. The $\alpha = 0$ means that the polaron state is extended along the whole system, such as the extended electron or hole state in the conventional inorganic semiconductors. In this case, it is obtained that the OMAR effect vanishes. The MR value will become larger with a stronger e–ph coupling whereas the polaron will be more localized, which explains why the MR value is usually much larger in OSCs than that in their inorganic counterparts.

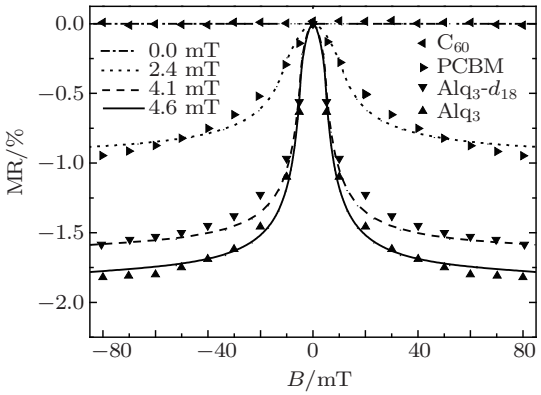


Fig. 20. The calculated dependence of MR on external magnetic field B under different hyperfine fields at $E = 0.001$ mV/Å (lines). The experimental results of MR measured by Rolfe *et al.*[119] and Nguyen *et al.*[120] are also shown for comparison (triangles).

Recently, Mahato *et al.* predicted an exceptionally large ($> 2000\%$) MR effect in one-dimensional, nonmagnetic systems. This effect was ascribed to the spin blockade in the one-dimensional electron transport.[107] Also Kersten *et al.* studied interchain hopping in polymers and found that the OMFE increases as the interchain hopping rate drops.[121] This kind of giant OMR cannot be explained by the above theory. Here, the coupling of polaron spin with the magnetic field or hyperfine interaction will be very intense due to the localization of the polaron state. Polaron hopping depends not only on the site (molecule) energy distribution but also on the spin orientation. For simplicity, we suppose that the charge and the spin hoppings are separate and the hopping rate is written as $W_{is,js'} = \alpha_{ss'}\omega_{ij}$, where ω_{ij} is the site energy dependent hopping rate described by the Marcus formula,[122] and α_{ss} is the probability that the polaron spin is conserved during hopping, while $\alpha_{s\bar{s}}$ ($\bar{s} = -s$) means that the spin flips. We have $\sum_{s} \alpha_{ss'} = 1$. Considering a polaron hopping between sites i and j, its spin is subjected to an external magnetic field and the local HFI. The Hamiltonian is written as

$$\hat{H} = g\mu_{\mathrm{B}}\hat{\boldsymbol{S}} \cdot \boldsymbol{B} + a_i\hat{\boldsymbol{S}} \cdot \hat{\boldsymbol{I}}_i + a_j\hat{\boldsymbol{S}} \cdot \hat{\boldsymbol{I}}_j, \tag{13}$$

where $\hat{\boldsymbol{S}}$ is the polaron spin operator, $\hat{\boldsymbol{I}}_i$ is the nuclear spin operator, and a_i is the strength of HFI at site i. The spin–orbit coupling is neglected because it is considered to be very weak in organic materials. To obtain probability $\alpha_{ss'}$, we consider the effect of different nuclear spin configurations $\left|s, \boldsymbol{I}_i, \boldsymbol{I}_j\right\rangle$ on the polaron spin and obtain the spin probability

$$\alpha_{ss'} = \begin{cases} \dfrac{B^2 + 7a_H^2/4}{B^2 + 9a_H^2/4}, & (s = s'), \\ \dfrac{a_H^2/2}{B^2 + 9a_H^2/4}, & (s \neq s'). \end{cases} \tag{14}$$

The hopping transport is described with the master equation (ME) method.[123,124] The ME has been proved to be an effective tool to explain experimentally observed mobility and presents a general framework to understand the transport of the disordered OSCs. When the spin is included, the ME is written as

$$\frac{\mathrm{d}P_{is}}{\mathrm{d}t} = \sum_{j \neq i, s'} \left[-W_{is,js'}P_{is}(1 - P_{js'}) + W_{js',is}P_{js'}(1 - P_{is})\right], \tag{15}$$

where P_{is} is the occupancy number of a polaron at site i with spin s. The mobility is given by

$$\mu = \frac{1}{PE} \sum_{is,js'} W_{is,js'}P_{is}(1 - P_{js'})R_{ij,x}.$$

By choosing suitable parameters, we calculate the dependence of the MC on the applied magnetic field. It is found that the theoretical result is quite consistent with the experimental data, as shown in Fig. 21. Therefore, strong spin-correlated hopping is the reason for the giant OMC. Recently, Mahato *et al.* predicted that the anisotropy of the molecular structure or conformation may have an apparent effect on the giant magnetic field effect. They obtained an exceptionally large MC value for an ideal one-dimensional transport.[107] Here we introduce the anisotropy of the OSC through a different hopping

integral in different direction by $\eta = t_\perp/t_0$, where t_0 expresses the hopping integral of polarons along the direction of the driving field, and $t_\perp$ is that along the vertical directions. The $\eta = 1$ means an isotropic OSC. The dependence of the MC on the anisotropy parameter η is shown in Fig. 22. It is found that the MC value increases with increasing anisotropy parameter. In the isotropic case ($\eta = 1$), the absolute value of MC is 62%. While in the quasi-one-dimensional transport ($\eta = 0.001$), the absolute value increases to 84%. The absolute value of the MC has an increment of about 30%. The physical mechanism is that the anisotropy will decrease the hopping routes of the polarons. Thus, the spin blocking effect will become apparent as a polaron does not easily hop to other molecules when it confronts to a spin-blocking or charge-blocking configuration in the transport direction. Our result is basically consistent with Kersten's Monte Carlo simulation.[121] Therefore, to get a large MC value, we suggest using organic materials with high-anisotropy structures or conformations.

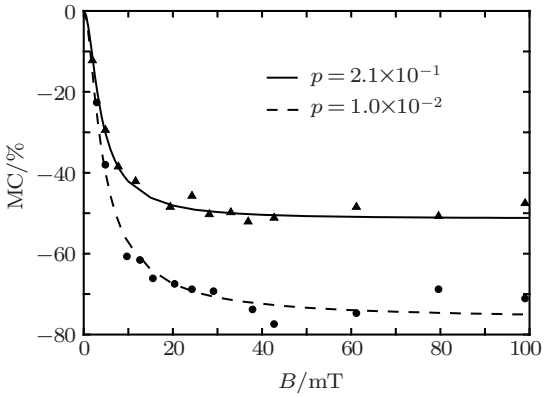


Fig. 21. Dependence of MC on B under different polaron densities. The experimental data (triangles and circles) are also shown for comparison.[99] The parameters are set as $\lambda = 0.07$ eV, $\sigma = 0.15$ eV, $t_0 = 0.01$ eV, $a_H = 1.5$ mT, $\gamma = 1$ nm^{-1}, and $T = 290$ K.

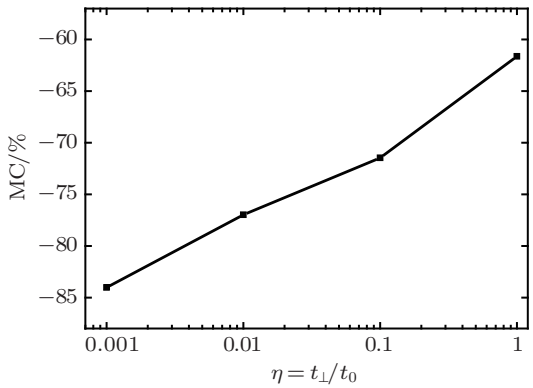


Fig. 22. Dependence of the MC on anisotropy parameter η with $B = 100$ mT. The parameters are set as $\lambda = 0.07$ eV, $\sigma = 0.15$ eV, $t_0 = 0.01$ eV, $p = 0.1$, $a_H = 1.5$ mT, $\gamma = 1$ nm^{-1}, and $T = 290$ K.

Si *et al.* presented a theory of OMAR based on the quenching of the quantum correlation between a carrier's spin and its local environment when the incoherent hopping takes place. They proved that this process contributes a spin-dependent prefactor to the attempt-to-escape frequency in the hopping rate, with its value modulated by the magnetic field. The resulting OMAR exhibits a positive Lorentzian saturation component and a negative small-field component, which are independent of the model's parameters.[125]

In 2010, Wang and Xie proposed an explanation of OMFE based on the charge-Lorentz effect instead of the spin-Zeeman effect.[126] They predicted that a non-symmetrical electronic orbit may result in an apparent change in transport when a magnetic field is applied. Later, in 2012, Alexandrov *et al.* also put forward hopping MC via nonzero orbital momentum.[127] They found that a weak magnetic field could shrink/expand the electronic p orbit. Their theory provides a plausible mechanism for a large low-field MR in disordered organic materials.

In the presence of a magnetic field, due to the charge-Lorentz effect, the transfer integral between molecule 1 and molecule 2 will be modified as

$$t = \frac{\hbar^2}{m}\int\left[\left(\psi_1^*\frac{\partial\psi_2}{\partial x} - \frac{\partial\psi_1^*}{\partial x}\psi_2\right) - \frac{2\mathrm{i}}{\phi_0}(\boldsymbol{A}\cdot\hat{\boldsymbol{x}})\psi_1^*\psi_2\right]\Big|_{x=d/2}\,\mathrm{d}y\mathrm{d}z, \tag{16}$$

where $\varphi_0 = c\hbar/e$ is the flux quanta. The integration is over the plane of $x = d/2$, midway between the two molecules. Obviously, the integral will be apparent if the molecules are asymmetrical about $y = 0$ or $z = 0$.

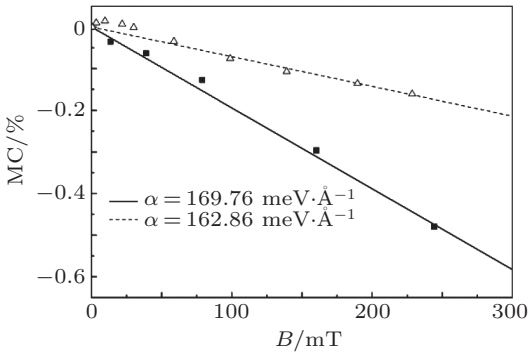


Fig. 23. Dependence of density-related MC on magnetic field. By setting a suitable e–ph coupling, the theoretical results fit the experimental data very well. (i) Square data of PtOEP are from Ref. [128] and the solid line is our theoretical result with $\alpha = 169.76$ meV$\cdot$Å^{-1}; (ii) triangle data of Ir(ppy)$_3$ are from Ref. [129] and dashed line is our theoretical result with $\alpha = 162.84$ meV$\cdot$Å^{-1}.

By considering the collision of a positive-charged polaron with a negative-charged one and the exciton formation in the organic layer through a non-adiabatic dynamic process, it is found that the exciton yield can be changed by applying a magnetic field due to the Lorentz effect on the wave function phase of the moving polarons. By calculating the current through the device and the MC, we obtain that the calculated MC is quite

consistent with some experimental observations. As shown in Fig. 23, it is also found that the MC value is sensitive to the asymmetrical structure and the e–ph coupling of the organic material, which explains why the magnetic effect in an OSC is much more apparent than that in its inorganic counterpart.[130]

5. Summary

During the past few years, more and more functional properties of organic materials have been revealed — electrical, magnetic, and optical. It is believed that practical spintronics will be achieved quite well in organic materials. Organic spintronics show interesting characteristics under electric, optical, magnetic, and thermal stimuli. In this article, we have only reviewed some snippets of this area, which include the spin characteristic of the carriers in organic materials, the transport of the spin-polarized current in them, and the effect of magnetism on the conductance of OSCs. The theoretical contributions of our group in spin polarization transport and OMFE were also presented. These investigations will be very helpful in finding more physical properties of OSCs and organic devices, and in initiating a variety of exciting new applications in organic spintronics.

Spin dependent phenomena in OSCs are different from their inorganic counterparts. The OSC characteristics include weak spin–orbit coupling as well as strong electron–phonon coupling. Even the seemingly insignificant hydrogen nuclear spin hyperfine interaction may give rise to some detectable effect. Organic materials are flexible, resource-rich, cheap, and much superior in these ways to the inorganic ones for applications in future electronic and spintronic devices. All these properties have motivated efforts to develop organic functional devices. Although the field is not progressing as swiftly as it could be (e.g., the experimental data are not consistent in some cases and the theoretical models are tailored to specific data), the enthusiasm in organic electronics and spintronics has been getting higher and higher. Recently, spin caloritronics has also been investigated in organic devices, which focuses on the interaction of spins with heat currents.[131] Thermoelectric and thermomagnetic effects are applied in thermometers, power generators, and coolers. The investigations include thermal conductance and spin-dependent Seebeck/Peltier coefficients, thermal spin-transfer torques, spin anomalous thermoelectric Hall effects, and so on. We believe that perseverance in investigating organic functional materials and organic devices will bring great advances in understanding the underlying mechanisms and in developing device applications in the organic world.

References

[1] Baibich M N, Broto J M, Fert A, Nguyen Van Dau F, Petroff F, Etienne P, Creuzet G, Friederich A and Chazelas J 1988 *Phys. Rev. Lett.* **61** 2472
[2] Bamas J, Fuss A, Camley R, Crunberg P and Zinn W 1990 *Phys. Rev. B* **42** 8110
[3] Wolf S A, Awschalom D D, Buhrman R A, Daughton J M, von Molnár S, Roukes M L, Chtchelkanova A Y and Treger D M 2001 *Science* **294** 1488
[4] Meservey R 1970 *Phys. Rev. Lett.* **25** 1270
[5] Johnson M and Silsbee R H 1985 *Phys. Rev. Lett.* **55** 1790
[6] Monzon F G, Tang H X and Roukes M L 2000 *Phys. Rev. Lett.* **84** 5022
[7] Friend R H, Gymer R W, Holmes A B, Burroughes J H, Marks R N, Taliani C, Bradley D D C, Santos D A Dos, Brédas J L, Lögdlund M and Salaneck W R 1999 *Nature* **397** 121
[8] Forrest S, Burrows P and Thompson M 2000 *IEEE Spectr.* **37** 29
[9] Voss D 2000 *Nature* **407** 442
[10] Naber W J M, Faez S and van der Wiel W G 2007 *J. Phys. D: Appl. Phys.* **40** R205
[11] Dediu V A, Hueso L E, Bergenti I and Taliani C 2009 *Nat. Mater.* **8** 707
[12] Alam K M and Pramanik S 2010 arXiv:1005.1118
[13] Xie S J, Ren J F, Fu J Y, Ahn K H, Smith D L, Bishop A R and Saxena A 2006 *Progress in Ferromagnetism Research* (New York: Nova Science Publishers, Inc.) pp. 67–84
[14] Ren J F, Hu G C, Zhang Y B, Lei J, Jiang H and Xie S J 2009 *Progress in Organic Spintronics*, Advances in condensed matter physics (Geelvinck S, ed.) (New York: Nova Science Publishers, Inc.) pp. 29–55
[15] Shirakawa H, Louis E J, MacDiarmid A G, Chiang C K and Heeger A J 1977 *J. Chem. Soc. Chem. Commun.* 578
[16] Tang C W and van Slyke S A 1987 *Appl. Phys. Lett.* **51** 913
[17] Burroughes J H, Bradley D D C, Brown A R, Marks R N, Mackay K, Friend R H, Burns P L and Holmes A B 1990 *Nature* **347** 539
[18] Sirringhaus H, Tessler N and Friend R H 1998 *Science* **280** 1741
[19] Ho P K H, Thomas D S, Friend R H and Tessler N 1999 *Science* **285** 233
[20] Tang C W and VanSlyke S A 1987 *Appl. Phys. Lett.* **51** 913
[21] Jiang Y Q, Peng Q, Gao X, Shuai Z G, Niu Y L and Lin S H 2012 *J. Mater. Chem.* **22** 4491
[22] Mataga N 1968 *Theor. Chim. Acta* **10** 372
[23] Korshak Y V, Medvedeva T V, Ovchinnikov A A and Spector V N 1987 *Nature* **326** 370
[24] Cao Y, Wang P, Hu Z, Li S Z, Zhang L Y and Zhao J G 1988 *Synth. Met.* **27** B625
[25] Miller J S, Epstein A J and Reiff W M 1988 *Chem. Rev.* **88** 201
[26] Zhao L and Yao K L 2000 *J. Phys.: Condens. Matter* **12** 5735
[27] Rajca A, Wongsriratanakul J and Rajca S 2001 *Science* **294** 1503
[28] Su W P, Schrieffer J R and Heeger A J 1979 *Phys. Rev. Lett.* **42** 1698
[29] Su W P, Schrieffer J R and Heeger A J 1980 *Phys. Rev. B* **22** 2209
[30] Su W P, Schrieffer J R and Heeger A J 1983 *Phys. Rev. B* **28** 1138
[31] Troisi A and Orlandi G 2006 *Phys. Rev. Lett.* **96** 086601
[32] Tarafder K, Sanyal B and Oppeneer P M 2010 *Phys. Rev. B* **82** 060413
[33] Hou D, Qiu J J, Xie S J and Saxena A 2013 *New J. Phys.* **15** 073044
[34] Han S X, Jiang H, Li X X and Xie S J 2014 *Org. Electron.* **15** 240
[35] Sanvito S 2007 *Nat. Mater.* **6** 803
[36] Boheme C and Lupton J 2013 *Nat. Nanotech.* **8** 612
[37] Zutic I, Fabian J and Sarma S D 2004 *Rev. Mod. Phys.* **76** 323
[38] Chen C D, Kuo W, Chung D S, Shyu J H and Wu C S 2002 *Phys. Rev. Lett.* **88** 047004
[39] Schmidt G, Ferrand D, Molenkamp L W, Filip A T and van Wees B J 2000 *Phys. Rev. B* **62** R4790
[40] Ohno Y, Young D K, Beschoten B, Matsukura F, Ohno H and Awschalom D D 1999 *Nature* **402** 790
[41] Fert A, George J M, Jaffrès H and Mattana R 2007 *IEEE Trans. Electron. Dev.* **54** 921
[42] Krinichnyi V I 2000 *Synth. Met.* **108** 173
[43] Jedema F J, Filip A T and van Wees B J 2001 *Nature* **410** 345
[44] Zhai H R 2013 *Spintronics* (Beijing: Science Press) (in Chinese)
[45] Rashba E I 1960 *Sov. Phys. Solid State* **2** 1109
[46] Bychkov Y A and Rashba E I 1984 *JETP Lett.* **39** 78
[47] Datta S and Das B 1990 *Appl. Phys. Lett.* **56** 665
[48] Dediu V, Murgia M, Matacotta F C, Taliani C and Barbanera S 2002 *Solid State Commun.* **122** 181
[49] Xiong Z H, Wu D, Vardeny Z V and Shi J 2004 *Nature* **427** 821
[50] Wu D, Xiong Z H, Li X G, Vardeny Z V and Shi J 2005 *Phys. Rev. Lett.* **95** 016802

[51] Majumdar S, Laiho R, Laukkanen P, Väyrynen I J, Majumdar H S and Österbacka R 2006 *Appl. Phys. Lett.* **89** 122114
[52] Dediu V, Hueso L E, Bergenti I, Riminucci A, Borgatti F, Graziosi P, Newby C, Casoli F, De Jong M P, Taliani C and Zhan Y 2008 *Phys. Rev. B* **78** 115203
[53] Mooser S, Cooper J F K, Banger K K, Wunderlich J and Sirringhaus H 2012 *Phys. Rev. B* **85** 235202
[54] Chen B B, Jiang S W, Ding H F, Jiang Z S and Wu D 2014 *Chin. Phys. B* **23** 018104
[55] Gobbi M, Golmar F, Llopis R, Casanova F and Hueso L E 2011 *Adv. Mater.* **23** 1609
[56] Cinchetti M, Heimer K, Wüstenberg J P, Andreyev O, Bauer M, Lach S, Ziegler C, Gao Y and Aeschlimann M 2009 *Nat. Mater.* **8** 115
[57] Drew A J, Hoppler J and Schulz L 2009 *Nat. Mater.* **8** 109
[58] Yu Z G 2011 *Phys. Rev. Lett.* **106** 106602
[59] Mott N F 1936 *Proc. R. Soc. London Ser. A* **153** 699
[60] Mott N F 1936 *Proc. R. Soc. London Ser. A* **156** 368
[61] Li S, Chen L S, George T H and Sun X 2004 *Phys. Rev. B* **70** 075201
[62] Xie S J, Ahn K H, Smith D L, Bishop A R and Saxena A 2003 *Phys. Rev. B* **67** 125202
[63] Fu J Y, Ren J F, Liu X J, Liu D S and Xie S J 2006 *Phys. Rev. B* **73** 195401
[64] Zwolak M and Ventra M D 2002 *Appl. Phys. Lett.* **81** 925
[65] Xie S J, Zhao J Q, Wei J H, Wang S G, Mei L M and Han S H 2000 *Europhys. Lett.* **50** 635
[66] Kikkawa J M and Awschalom D D 1999 *Nature* **397** 139
[67] Hanbicki A T, Jonker B T, Itskos G, Kioseoglou G and Petrou A 2002 *Appl. Phys. Lett.* **80** 1240
[68] Strěda P and Šeba P 2003 *Phys. Rev. Lett.* **90** 256601
[69] Lee H C and Eric Yang S R 2005 *Phys. Rev. B* **72** 245338
[70] Mireles F and Kirczenow G 2001 *Phys. Rev. B* **64** 024426
[71] Sun Q F, Wang J and Guo H 2005 *Phys. Rev. B* **71** 165310
[72] Lei J, Li H, Yin S and Xie S J 2008 *J. Phys.: Condens. Matter* **20** 095201
[73] Rashba E I 2000 *Phys. Rev. B* **62** R16267
[74] Schmidt G, Ferrand D, Molenkamp L W, Filip A T and van Wees B J 2000 *Phys. Rev. B* **62** R4790
[75] Schmidt G, Molenkamp L W and Bauer G W 2001 *Materials Science and Engineering C* **15** 83
[76] Schmidt G and Molenkamp L W 2001 *J. Appl. Phys.* **89** 7443
[77] Schmidt G, Richter G, Grabs P, Gould C, Ferrand D and Molenkamp LW 2001 *Phys. Rev. Lett.* **87** 227203
[78] Smith D L and Silver R N 2001 *Phys. Rev. B* **64** 045323
[79] Albrecht J D and Smith D L 2002 *Phys. Rev. B* **66** 113303
[80] Fert A and Jaffres H 2002 *Phys. Rev. B* **64** 184420
[81] Yu Z G and Flatte M E P 2002 *Phys. Rev. B* **66** 235302
[82] Agrawal S, Jalil M B A, Teo K L and Liew Y F 2005 *J. Appl. Phys.* **97** 103907
[83] Ruden P P and Smith D L 2004 *J. Appl. Phys.* **95** 4898
[84] Yu Z G, Berding M A and Krishnamurthy S 2005 *J. Appl. Phys.* **97** 024510
[85] Yu Z G, Berding M A and Krishnamurthy S 2005 *Phys. Rev. B* **71** 060408
[86] Scott J C, Pfluger P, Krounbi M T and Street G B 1983 *Phys. Rev. B* **28** 2140
[87] Genoud F, Guglielmi M, Nechtschein M, Genies E and Salmon M 1985 *Phys. Rev. Lett.* **55** 118
[88] e Silva G M 2000 *Phys. Rev. B* **61** 10777
[89] Ren J F, Fu J Y, Liu D S, Mei L M and Xie S J 2005 *J. Phys.: Condens. Matter* **17** 2341
[90] Ren J F, Fu J Y, Liu D S, Mei L M and Xie S J 2005 *J. Appl. Phys.* **98** 074503
[91] Zhang Y B, Ren J F, Hu G C and Xie S J 2008 *Org. Electron.* **9** 687
[92] Hu B, Yan L and Shao M 2009 *Adv. Mater.* **21** 1500
[93] Davis A H and Bussmann K 2004 *J. Vac. Sci. Technol. A* **22** 1885
[94] Francis T L, Mermer Ö, Veeraraghavan G and Wohlgenannt M 2004 *New J. Phys.* **6** 185
[95] Mermer Ö, Veeraraghavan G, Francis T L, Sheng Y, Nguyen D T, Wohlgenannt M, Kohler A, Al-Suti M K and Khan M S 2005 *Phys. Rev. B* **72** 205202
[96] Shakya P, Desai P, Somerton M, Gannaway G, Kreouzis T and Gillin W P 2008 *J. Appl. Phys.* **103** 103715
[97] Martin J L, Bergeson J D, Prigodin V N and Epstein A J 2010 *Synth. Met.* **160** 291
[98] Kang H, Park C H, Lim J, Lee C, Kang W and Yoon C S 2012 *Org. Electron.* **13** 1012
[99] Desai P, Shakya P, Kreouzis T and Gillin W P 2007 *Phys. Rev. B* **76** 235202
[100] Wang F J, Bässler H and Vardeny Z V 2008 *Phys. Rev. Lett.* **101** 236805
[101] Bloom F L, Wagemans W and Koopmans B 2008 *J. Appl. Phys.* **103** 07F320
[102] Bergeson J D, Prigodin V N, Lincoln D M and Epstein A J 2008 *Phys. Rev. Lett.* **100** 067201
[103] Kang H, Lee I J and Yoon C S 2012 *Appl. Phys. Lett.* **100** 073302
[104] Mermer Ö, Veeraraghavan G, Francis T L and Wohlgenannt M 2005 *Solid State Commun.* **134** 631
[105] Nguyen T D, Markosian G H, Wang F, Wojcik L, Li X G, Ehrenfreund E and Vardeny Z V 2010 *Nat. Mater.* **9** 345
[106] Zhang Q M, Lei Y L, Jia W Y, Chen L J, Zhang Y, Yang X H, You Y T and Xiong Z H 2013 *Org. Electron.* **14** 2875
[107] Mahato R N, Lülf H, Siekman M H, Kersten S P, Bobbert P A, Jong M P de, Cola L De and van der Wiel W G 2013 *Science* **341** 257
[108] Boheme C and Lupton J 2013 *Nat. Nanotech.* **8** 612
[109] Yu Z G, Ding F Z and Wang H B 2013 *Phys. Rev. B* **87** 205446
[110] Nguyena T D, Sheng Y, Rybicki J, Veeraraghavan G and Wohlgenannta M 2010 *Synth. Met.* **160** 320
[111] Veeraraghavan G, Nguyen T D, Sheng Y, Mermer Ö and Wohlgenannt M 2007 *J. Phys.: Condens. Matter* **19** 036209
[112] Ding B F, Yao Y, Sun Z Y, Wu C Q, Gao X D, Wang Z J, Ding X M, Choy W C H and Hou X Y 2010 *Appl. Phys. Lett.* **97** 163302
[113] Majumdar S, Majumdar H S, Aarnio H, Vanderzande D, Laiho R and Österbacka R 2009 *Phys. Rev. B* **79** 201202
[114] Bobbert P A, Nguyen T D, Oost F W A van, Koopmans B and Wohlgenannt M 2007 *Phys. Rev. Lett.* **99** 216801
[115] Desai P, Shakya P, Kreouzis T and Gillin W P 2007 *Phys. Rev. B* **75** 094423
[116] Liu R, Zhang Y, Lei Y L, Chen P and Xiong Z H 2009 *J. Appl. Phys.* **105** 093719
[117] Qin W, Yin S, Gao K and Xie S J 2012 *Appl. Phys. Lett.* **100** 233304
[118] Li X X, Dong X F, Lei J, Xie S J and Saxena A 2012 *Appl. Phys. Lett.* **100** 142408
[119] Rolfe N J, Heeney M, Wyatt P B, Drew A J, Kreouzis T and Gillin W P 2009 *Phys. Rev. B* **80** 241201
[120] Nguyen T D, Sheng Y, Wohlgenannt M and Anthopoulos T D 2007 *Synth. Met.* **157** 930
[121] Kersten S P, Meskers S C J and Bobbert P A 2012 *Phys. Rev. B* **86** 045210
[122] Marcus R A 1993 *Rev. Mod. Phys.* **65** 599
[123] Yu Z G, Smith D L, Saxena A, Martin R L and Bishop A R 2001 *Phys. Rev. B* **63** 085202
[124] Pasveer W F, Cottaar J, Tanase C, Coehoorn R, Bobbert P A, Blom P W M, de Leeuw D M and Michels M A J 2005 *Phys. Rev. Lett.* **94** 206601
[125] Si W, Yao Y, Hou X Y and Wu C Q 2014 *Org. Electron.* **15** 824
[126] Wang X R and Xie S J 2010 *Europhys. Lett.* **92** 57013
[127] Alexandrov A S, Dediu V A and Kabanov V V 2012 *Phys. Rev. Lett.* **108** 186601
[128] Nguyen T D, Sheng Y, Rybicki J, Veeraraghavan G and Wohlgenannt M 2007 *J. Mater. Chem.* **17** 1995
[129] Sheng Y, Nguyen T D, Veeraraghavan G, Mermer Ö and Wohlgenannt M 2007 *Phy. Rev. B* **75** 035202
[130] Li S Z, Dong X F, Yi D and Xie S J 2013 *Org. Electron.* **14** 2216
[131] Bauer G E W, Saitoh E and Wees B J van 2012 *Nat. Mater.* **11** 391